Kvazari sa visokom stopom akrecije
Da li možemo da ih koristimo kao standardne sveće?

Nataša Bon[1]

“Extreme Team”

Paola Marziani[2], Edi Bon[1],
C.A. Negrete[3] , D. Dultzin[3] , A. del Olmo[4], M. D’Onofrio[5],
M.L. Martínez-Aldama[4,6]

1 Astronomical Observatory, Belgrade, Volgina 7, 11160, Belgrade, Serbia

2 INAF, Osservatorio Astronomico di Padova, IT 35122, Padova, Italy

3 Instituto de Astronomía, UNAM, Mexico D.F. 04510, Mexico

4 Instituto de Astronomía, UNAM, Mexico D.F. 04510, Mexico

5 Instituto de Astrofisíca de Andalucía, IAA-CSIC, E-18008 Granada, Spain

6 Center for Theoretical Physics, Polish Academy of Sciences, Al. Lotnikow 32/46, Warsaw, Poland

MODERNA VERZIJA HABLOVOG DIJAGRAMA – SN Ia

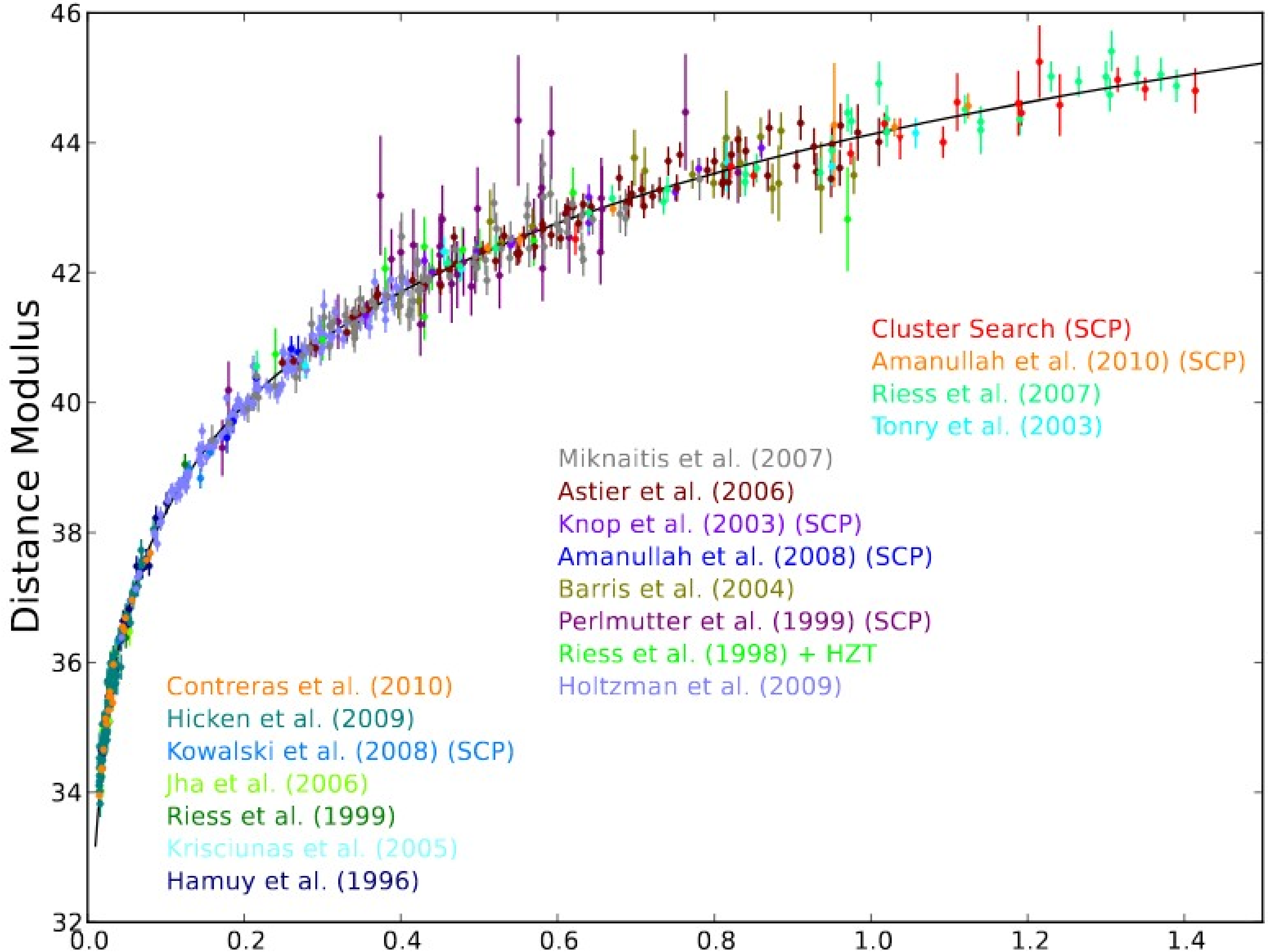

Suzuki +, 2013, ApJ 746, 24

Negrete, A. & Extreme Team A&A, 2018, 620,118

KVAZARI KAO STANDARNE SVECE?

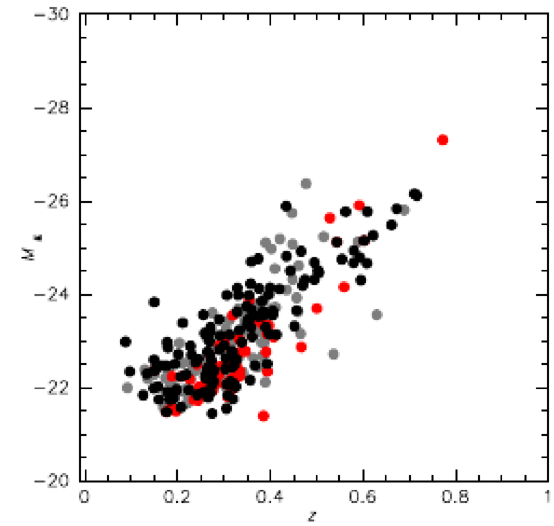

Fig. 3. Hubble diagram M_g vs. z for the 302 sources analyzed in this paper. Black circles: cosmo sample, grey circles: Pop. A not belonging to cosmo sample, red circles: Population. B. The cross indicates the average error.

ZA – OSOBINE KOJE IH ČINE POTENCIJALNIM STANDARDNIM SVEĆAMA:
- DO SADA OTKRIVENO VIŠE OD 200.000 KVAZARA
- VEOMA LUMINOZNI OBJEKTI
- DETEKTOVANI U RANIM EPOHAMA UNIVERZUMA (z ~7)

PROTIV:
-VEOMA SE RAZLIKUJU PO LUMINOZNOSTI I SEDu
-VELIKE PROMENJIVOSTI
-VELIKE RAZLIKE U FIZIČKIM USLOVIMA CENTRALNOG REGIONA – ŠIROKI SPEKTAR OSOBINA NA SVIM TALASNIM DUŽINAMA
-

CILJ JE PRONACI JEDAN ILI VISE PARAMETARA USKO VEZANIH SA LUMINOZNOSCU KVAZARA – IZOLOVATI KLASU KVAZARA SA KONSTANTNOM KARAKTERISTIKOM, NA OSNOVU KOJE JE MOGUCE ODREDITI LUMINOZNOST KVAZARA, NEZAVISNO OD CRVENOG POMAKA

KORACI-SELEKTOVATI - TACKASTE OBJEKTE – VISE LUMINOZNOSTI
- PLAVE OBJEKTE – KOREKCIJA POCRVENJENJA I - VISOK S/N U X-DOMENU
- HOMOGEN UZORAK – U SMISLU SEDa

UVOD – SISTEMATIZACIJA KVAZARA

Quasars lack stars' spherical symmetry.

Type 1 AGN are mainly unobscured accretors, probably seen at a viewing angle in between 0°/a few degrees and 45°-60° from the accretion disk axis.

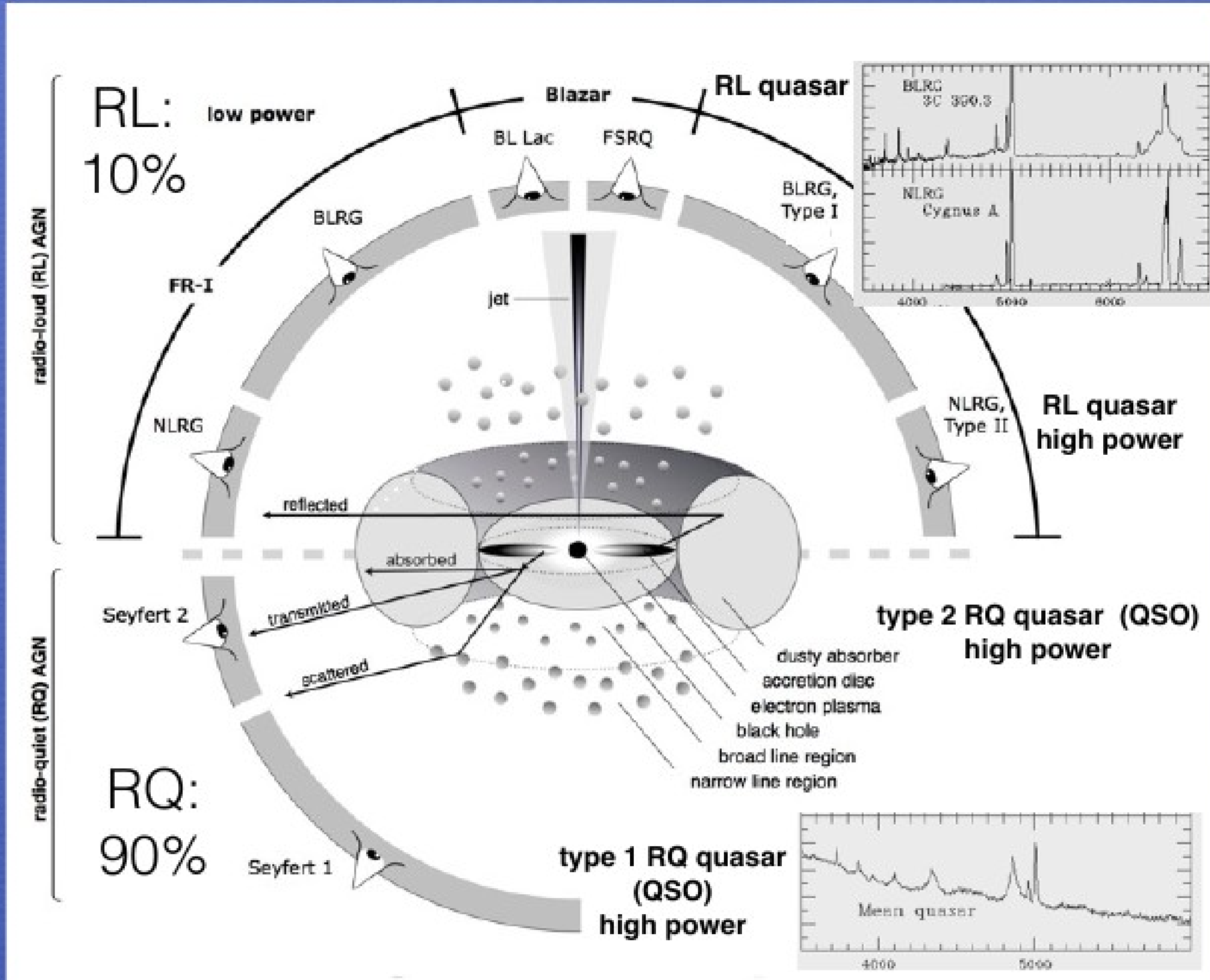

Adapted from
Beckmann & Shrader 2013

UVOD - RAZLICITOSTI KVAZARA

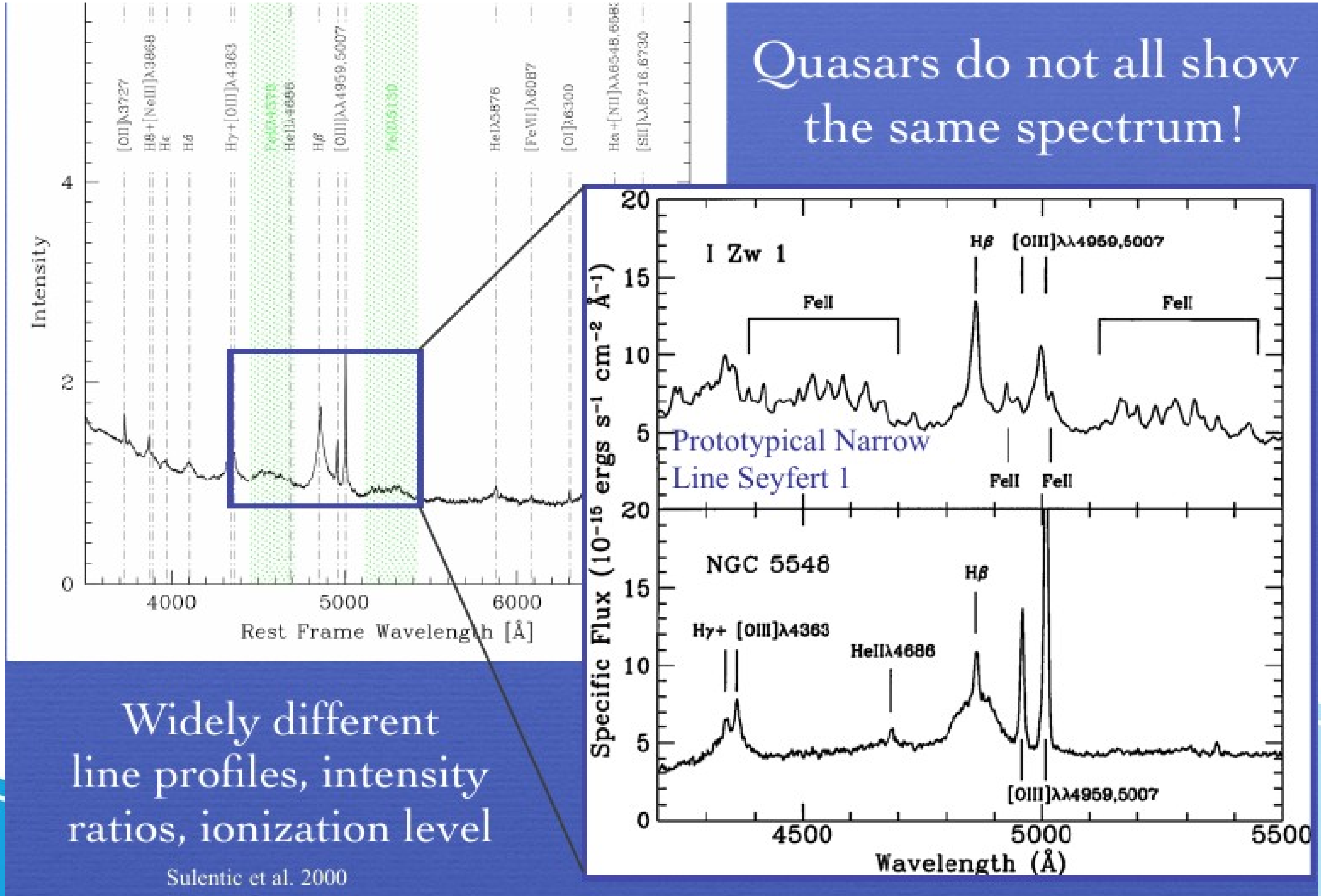

UVOD – USREDNJENI SPEKTRI KVAZARA TIPA 1

Quasars' optical and UV spectrum from the Sloan DSS: broad and narrow lines emitted by ionic species over a wide range of IPs

	Broad	Narrow
High Ionization	CIVλ1549, HeII	[OIII]λλ4959,5007, HeII,NeIII
Low Ionization	Balmer (Hβ), FeII, MgIIλ2800, CaII IR Triplet)	Balmer, [OI]λ6300,

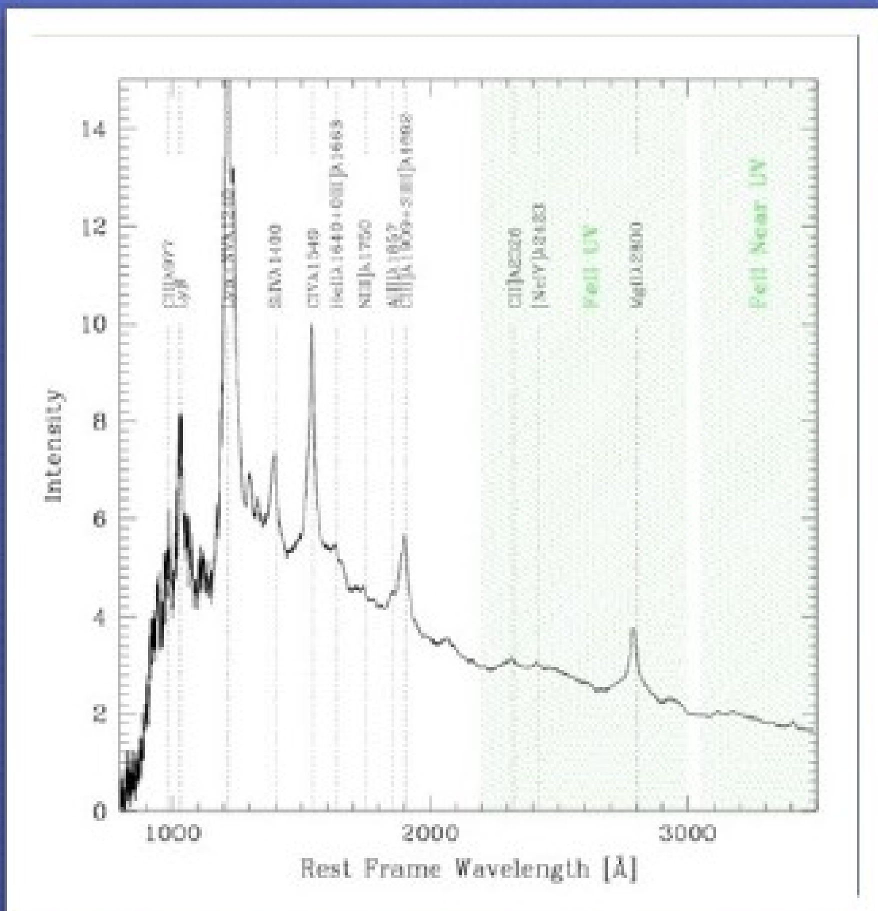

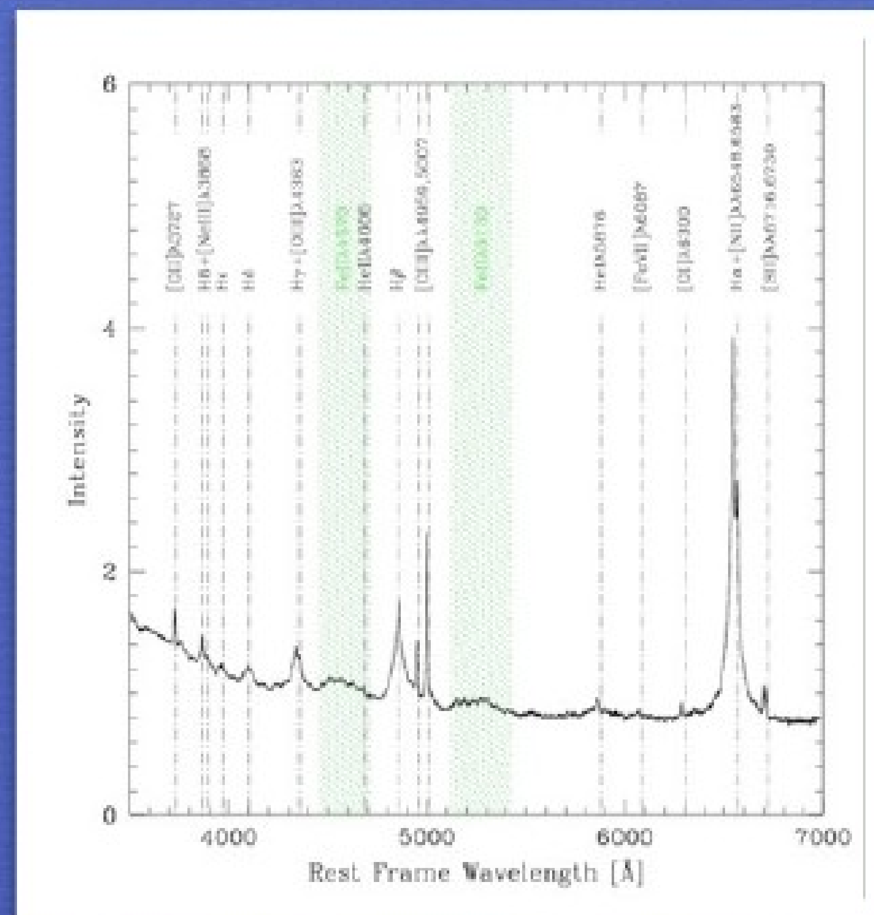

The composite quasar spectrum from the Sloan DSS (Van den Berk et al. 2001; Marziani et al. 2006)

"Main Sequence of Quasars"

Efforts to organize Type 1 AGNs into the "main sequence" of quasars, that allows to set observational constraints on dynamics and physical conditions within BLR.

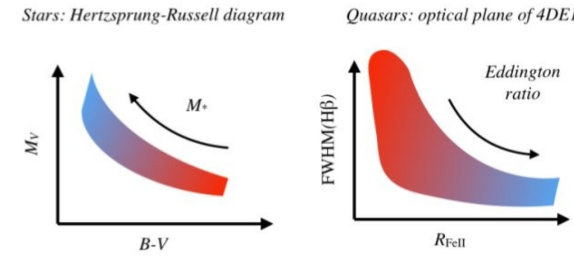

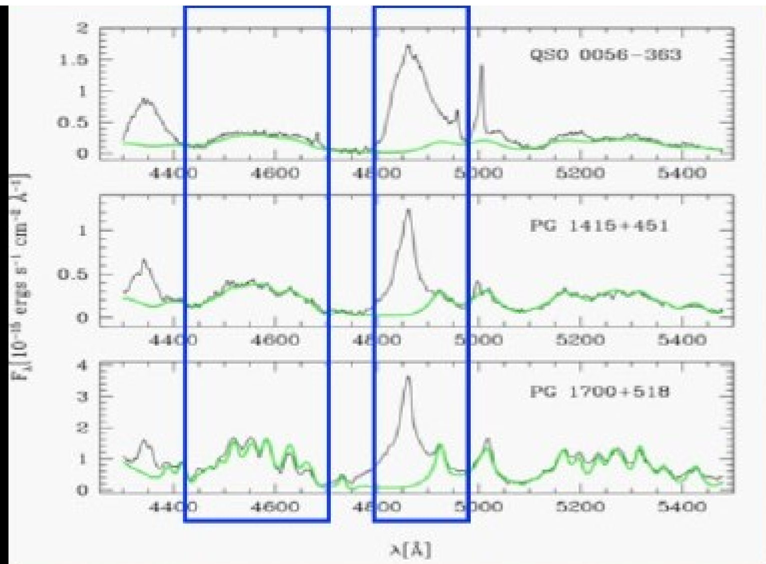

$$R_{\rm FeII} = \frac{I({\rm FeII}\lambda4570)}{I(H\beta)} \approx \frac{W({\rm FeII}\lambda4570)}{W(H\beta)}$$

Marziani +, MNRAS 2010, 409, 1033

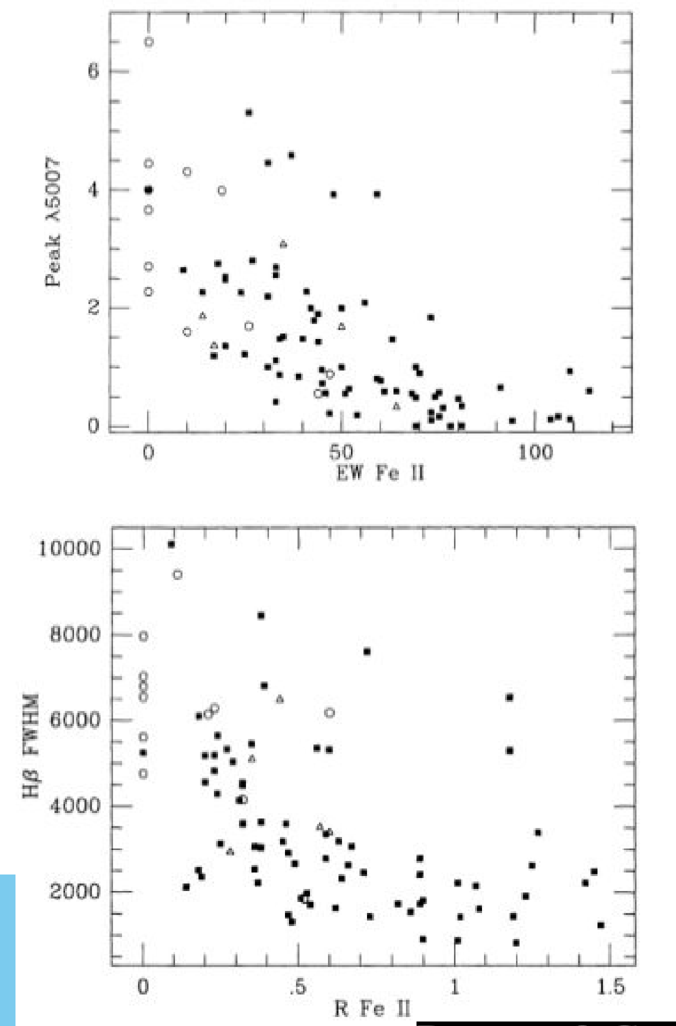

Boroson & Green, 1992

“Main Sequence of Quasars”

There were many efforts to organize Type 1 AGNs into the “main sequence” of quasars, that allows to set observational constraints on dynamics and physical conditions within BLR.

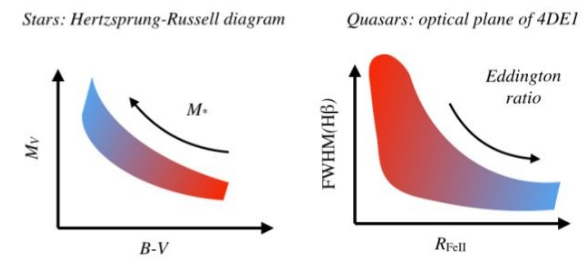

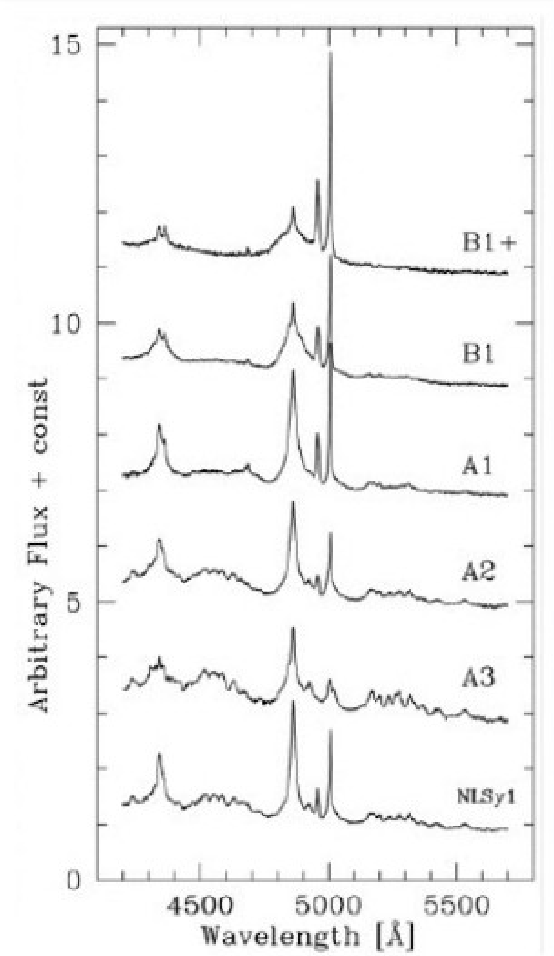

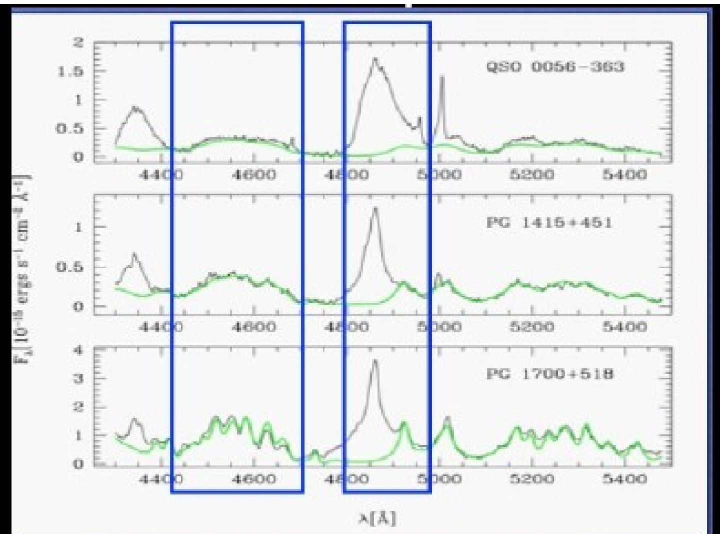

$$R_{\mathrm{FeII}} = \frac{I(\mathrm{FeII}\lambda4570)}{I(H\beta)} \approx \frac{W(\mathrm{FeII}\lambda4570)}{W(H\beta)}$$

Marziani +, MNRAS 2010, 409, 1033

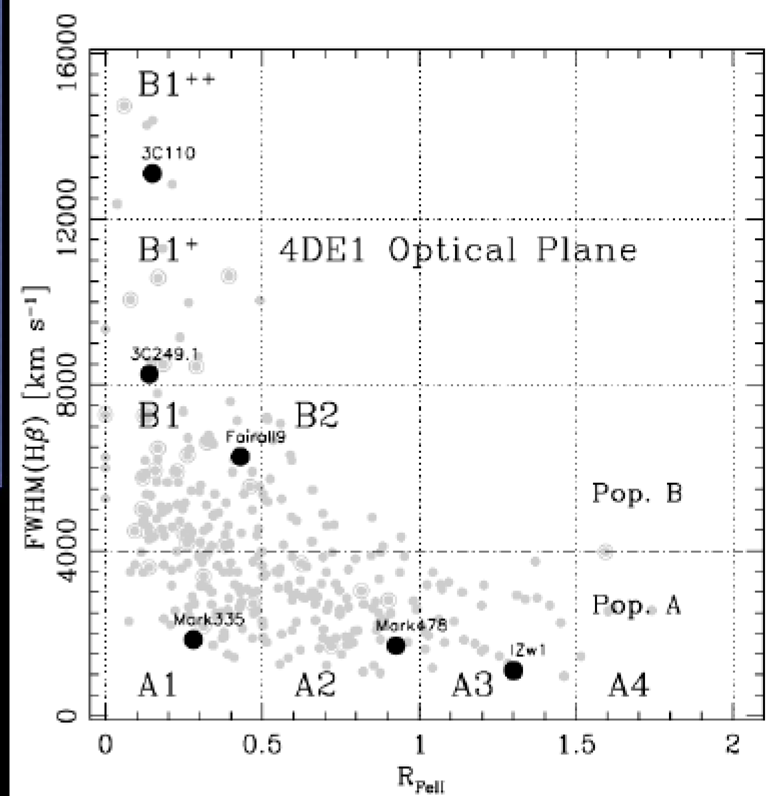

GLAVNI NIZ KVAZARA TIPA 1

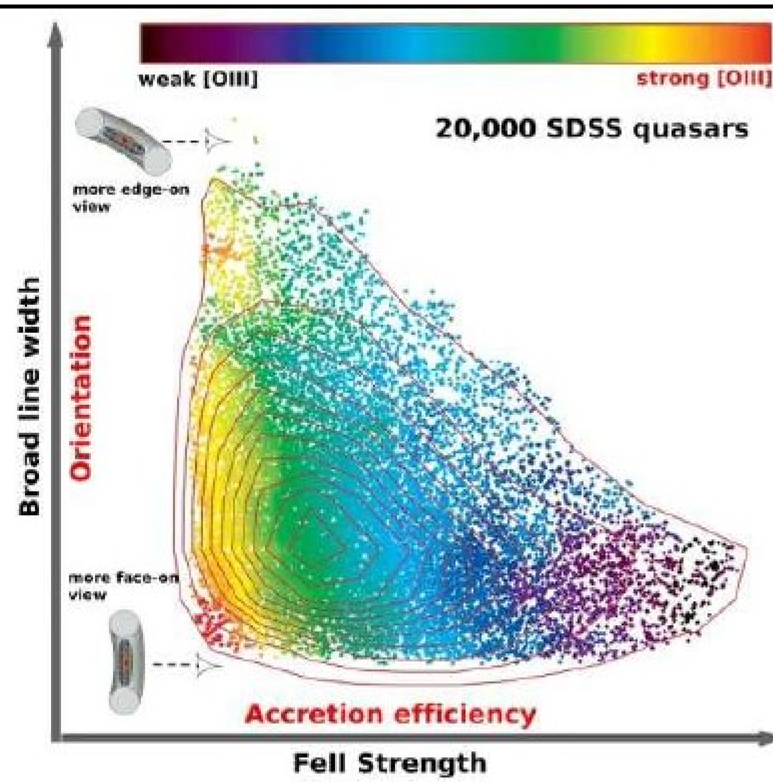

Shen & Ho, 2014

FeII emission is self-similar but intensity with respect to Hβ changes from object to object

FeII emission from UV to the IR can dominate the thermal balance of the low-ionization BLR

Marinello et al. 2018

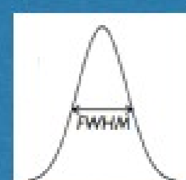

FWHM(Hβ): related to the velocity field in the low-ionization BLR (predominantly virialized)

Peterson & Wandel 2000; recent reverberation studies

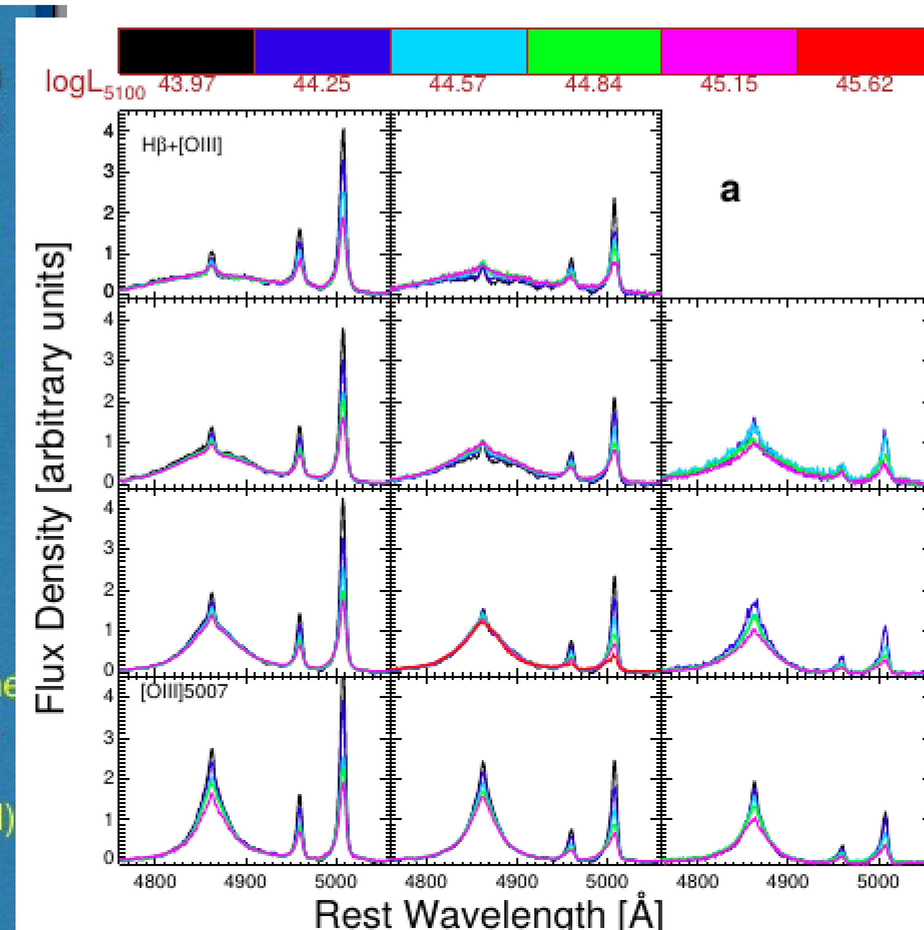

GLAVNI NIZ KVAZARA TIPA 1

The CIVλ1549 and Hβ line profiles: low-ionization symmetric and unshifted and high ionization blueshifted components coexisting even at the highest luminosities

➜ A virialized, flattened subsystem emitting Hβ and low-ionization line + a subsystem due to winds or outflows

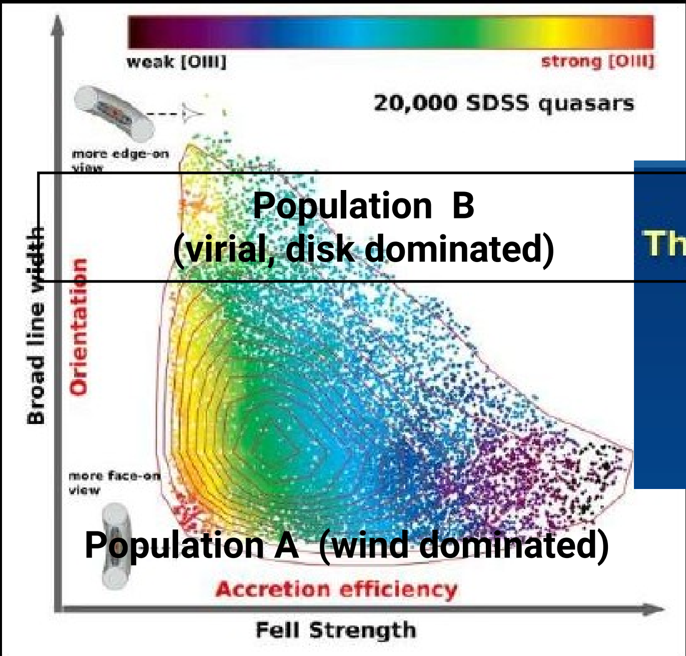

Shen & Ho, 2014

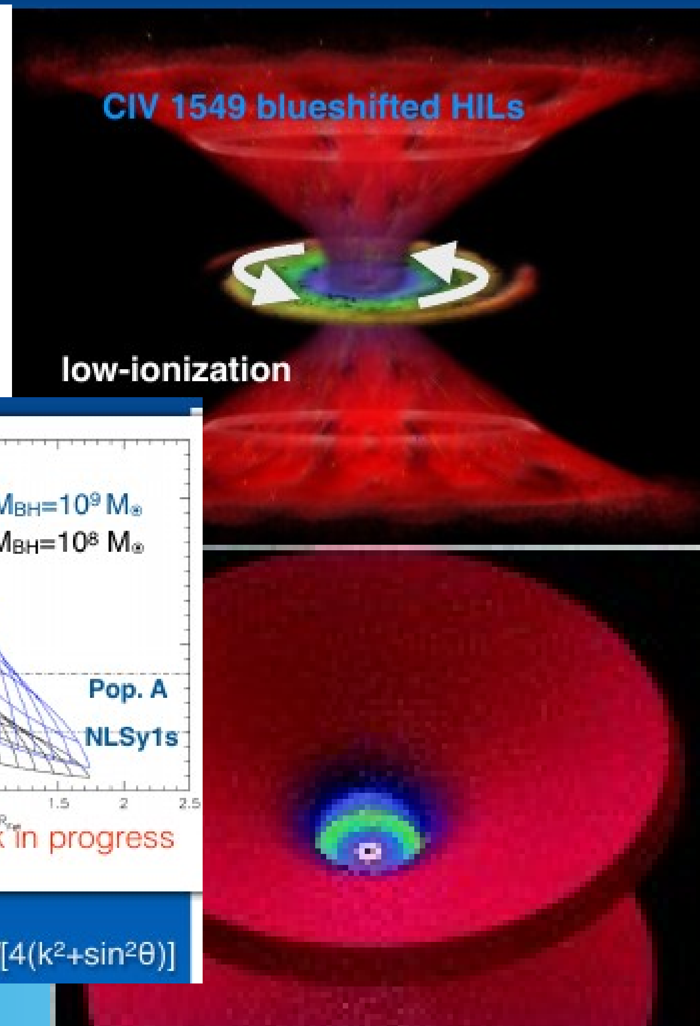

Elvis, 2000

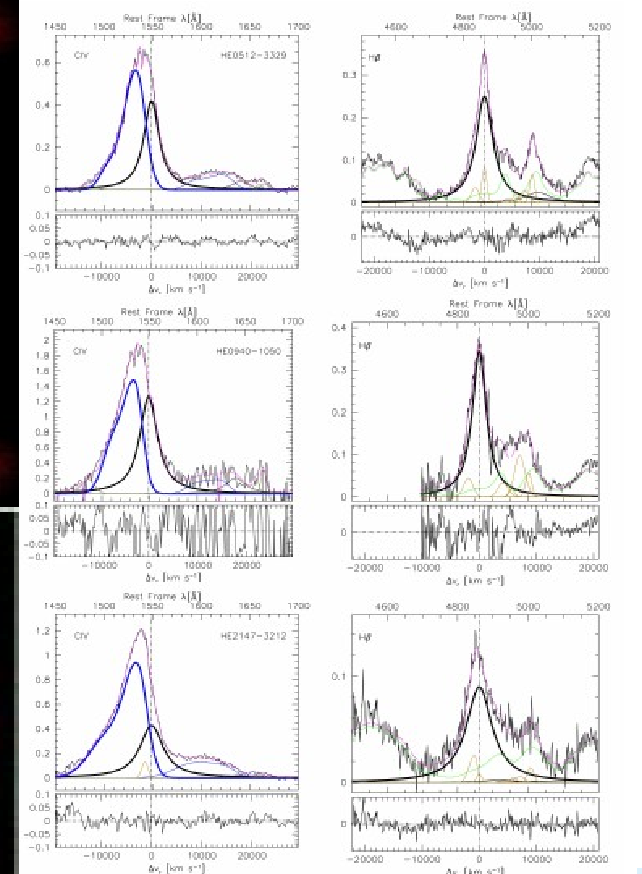

$L>10^{47}$ erg s^{-1}: extremely high amplitude blueshifts in CIV 1549 profiles of Hamburg-ESO Pop. A quasars; Sulentic et al. 2017

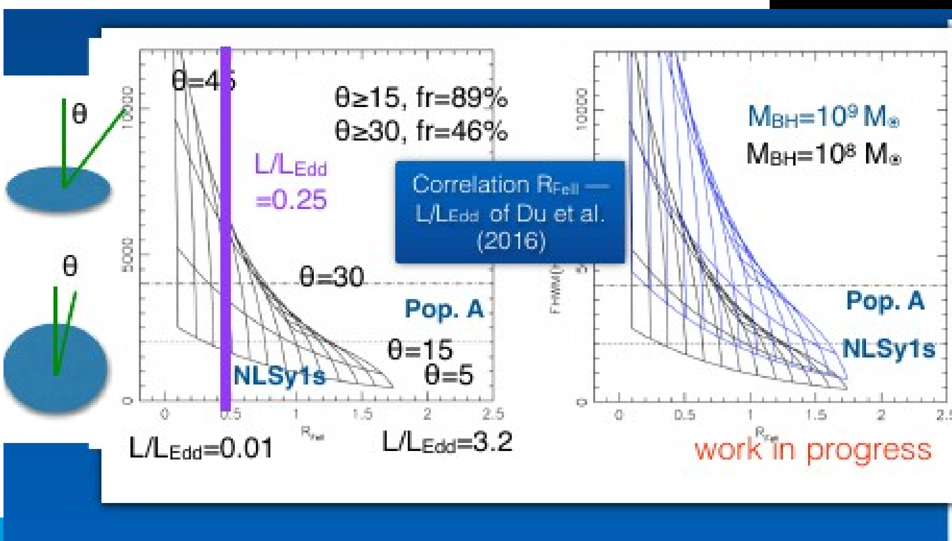

virial $M_{BH} \Rightarrow$ FWHM $\propto M_{BH}^{1/4} (L/L_{Edd})^{-1/4} f(\theta)^{-1/2}$; $f(\theta)=1/[4(k^2+\sin^2\theta)]$

4DE1 PROSTOR PARAMETARA (SULENTIC, MARZIANI, DULTZIN,2000)

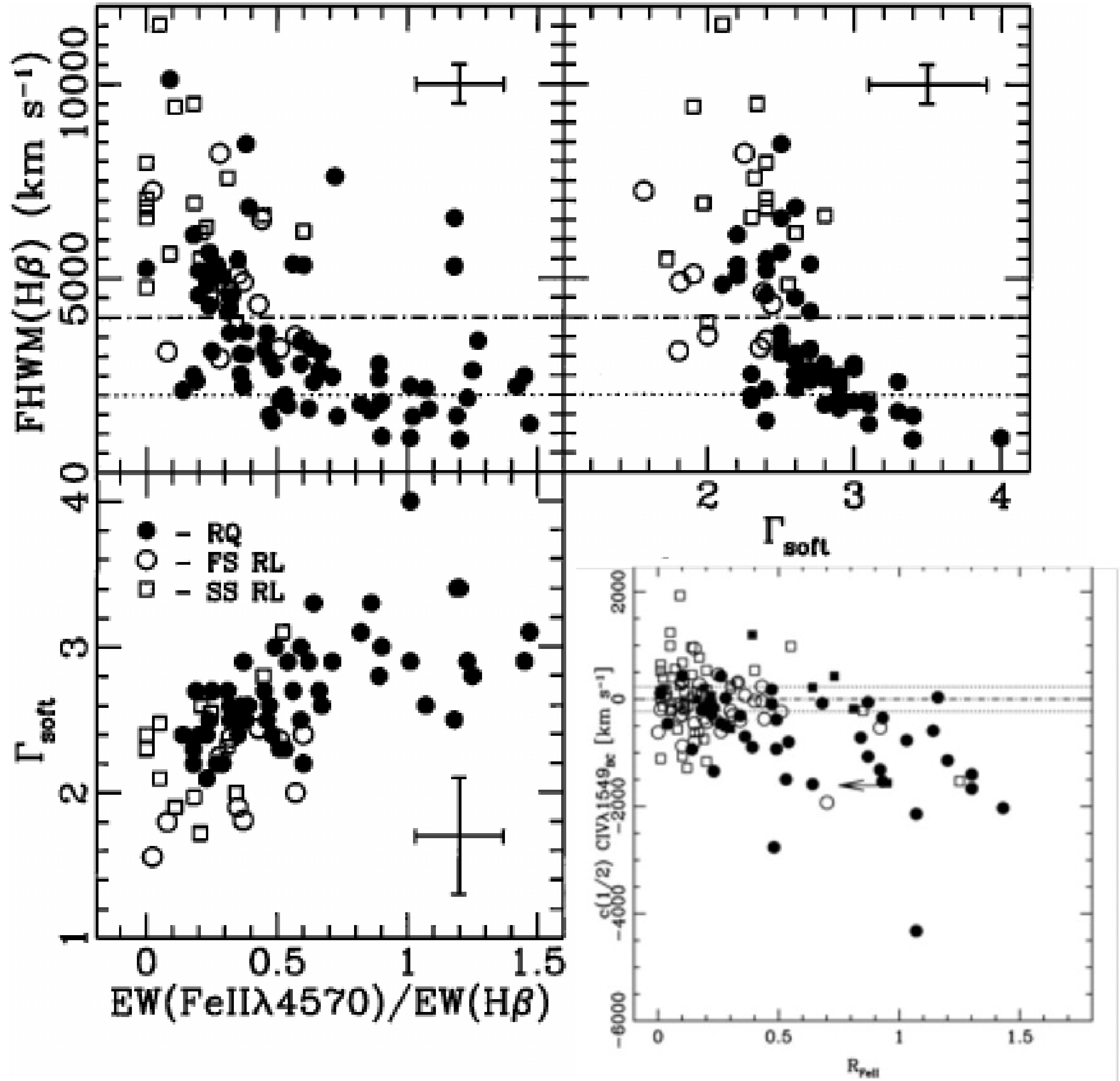

GLAVNI NIZ KVAZARA TIPA 1

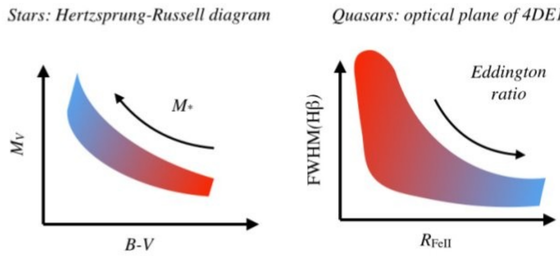

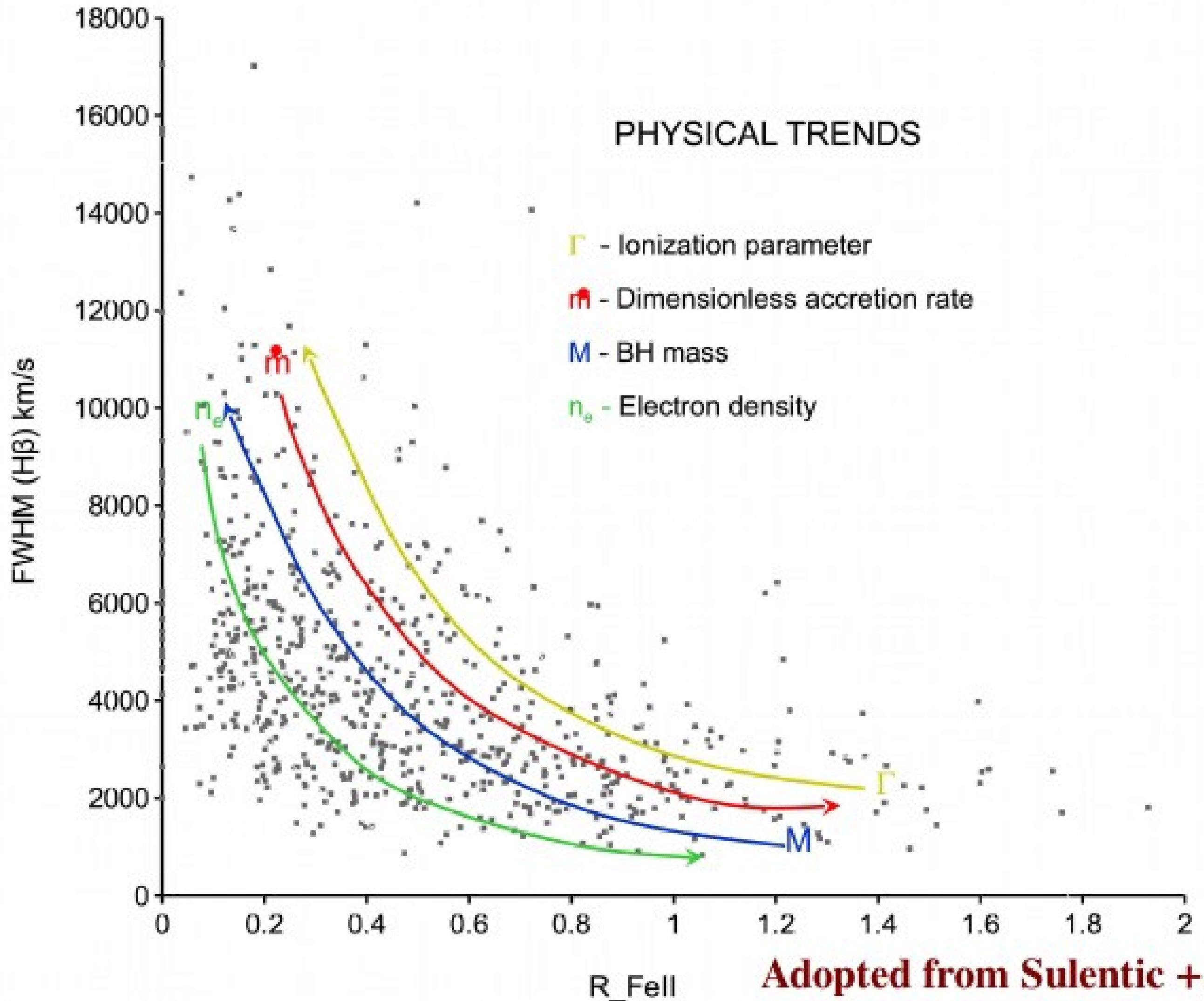

Adopted from Sulentic +, 2014

VEZA IZMEĐU R_{FeII} I L/L_{Edd}

The MBH proxy σ_* decreases with R_{FeII} in narrow luminosity bins =>

L/L_{Edd} increases with R_{FeII}

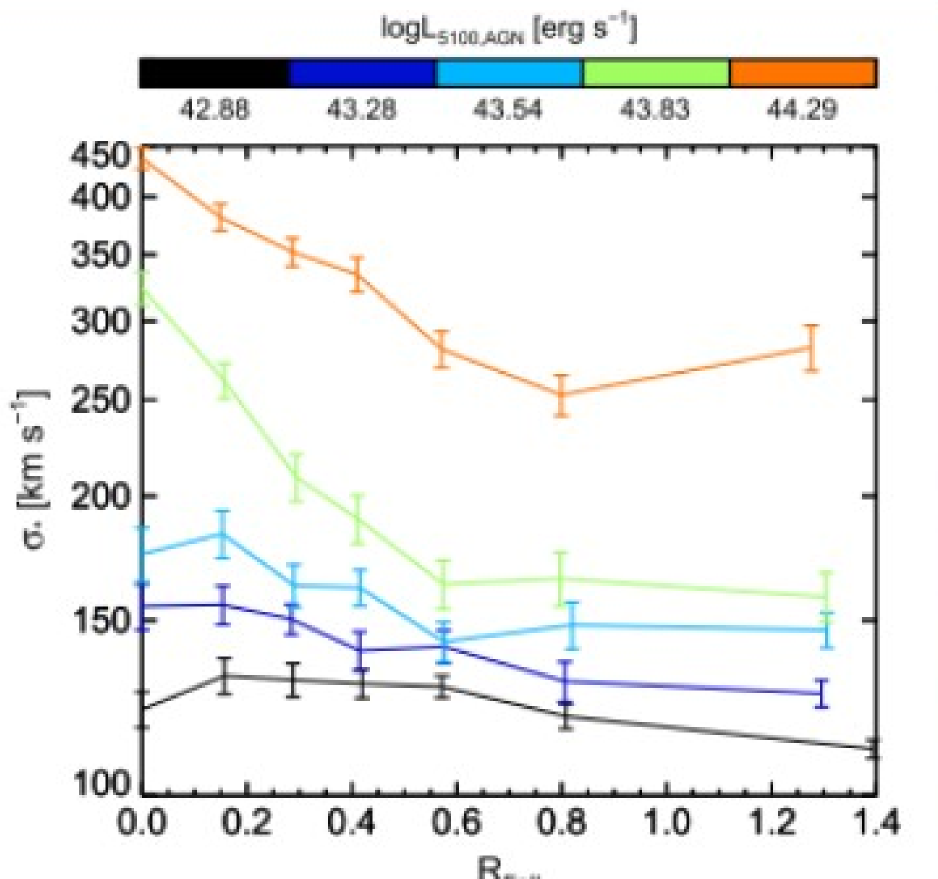

Fundamental plane of accreting massive black holes for reverberation-mapped AGN => $R_{FeII} > 1$ => $L/L_{Edd} > 1$

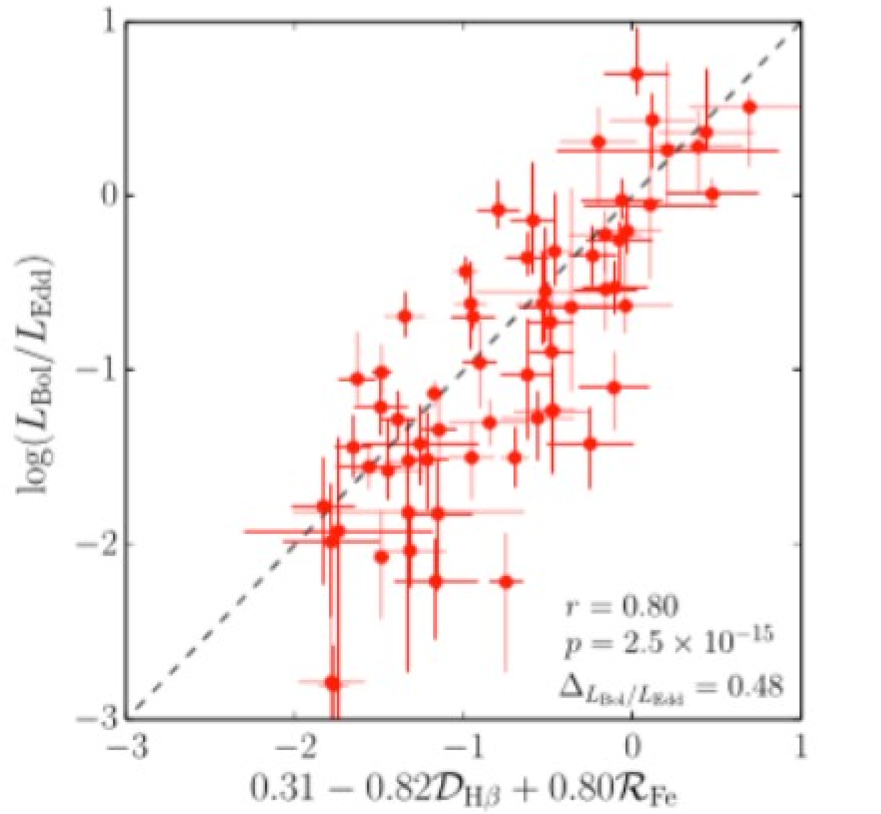

$$\log\left(\dot{\mathscr{M}}, L_{\rm bol}/L_{\rm Edd}\right) = \alpha_k + \beta_k \mathcal{D}_{\rm H\beta} + \gamma_k \mathcal{R}_{\rm Fe},$$

$$\mathcal{D}_{\rm H\beta} = \frac{\rm FWHM}{\sigma_{\rm H\beta}},$$

Sun & Shen, 2015

Du+, 2016, assuming virial relation

EXTREMNA POPULACIJA A – SELEKCIJA I FIZICKI USLOVI

Extreme Population A (xA) quasars satisfy $R_{FeII} > 1$; ~ 10% of quasars in low-z, optically selected samples

xA quasars show distinctive features: **unreddened, often "weak-lined quasars (W(CIVλ1549)≤10Å)" Prominent AlIIIλ1860, very weak CIII]λ1909 allow for easy UV selection criteria.**

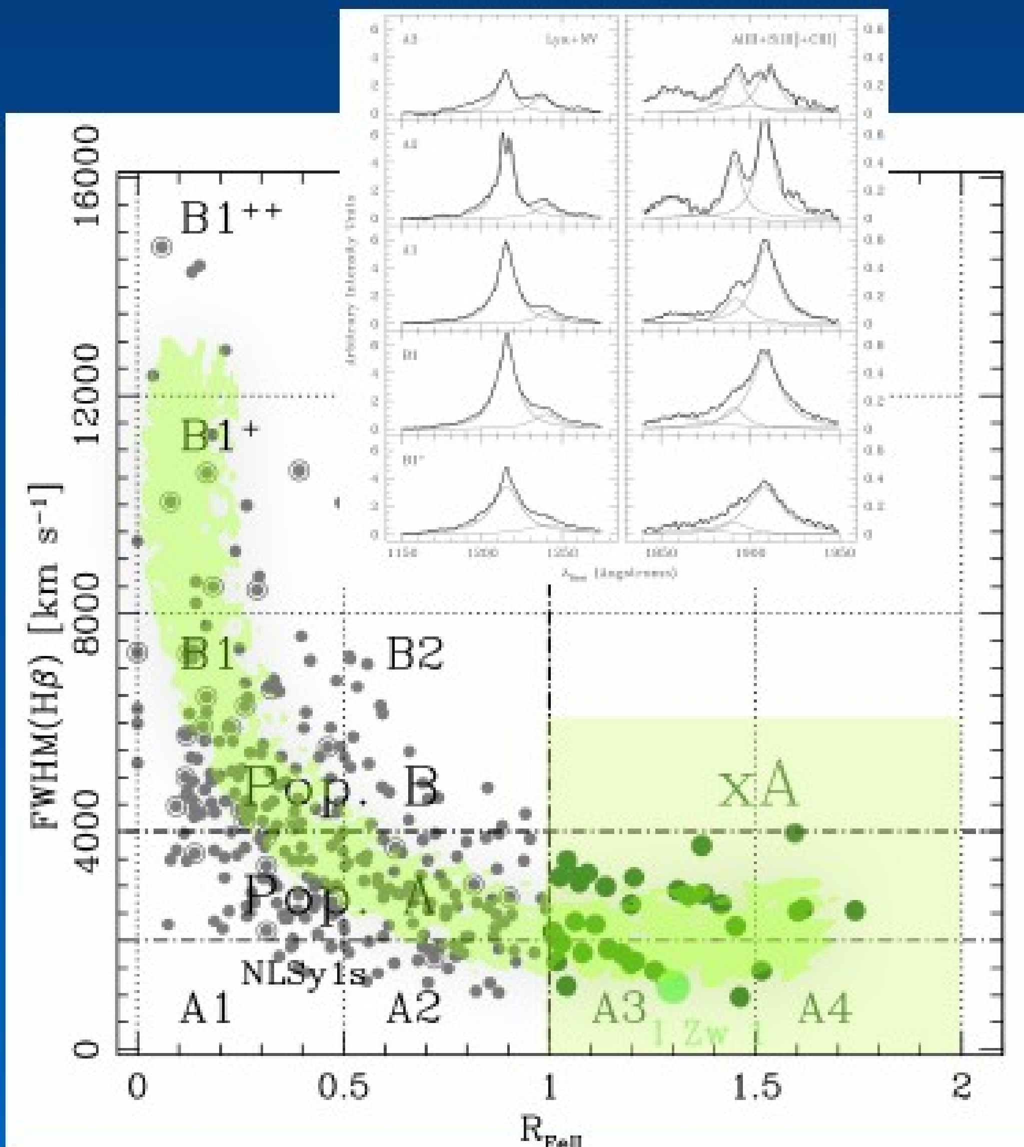

Negrete et al. 2018; Martinez-Aldama et al. 2018 (z>2)

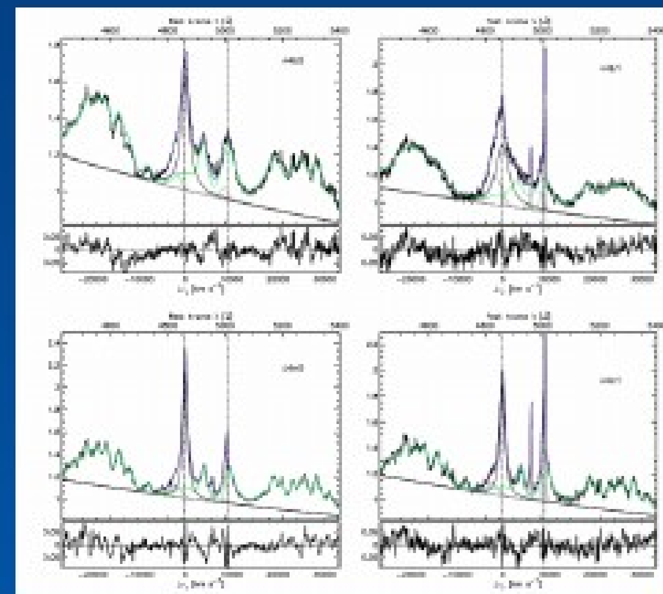

Selection criteria from line intensity ratios

1) R_{FeII} = FeIIλ4570 blend/Hβ > 1.0

2) UV AlIII λ1860/SiIII]λ1892>0.5 & SiIII]λ1892/CIII]λ1909>1

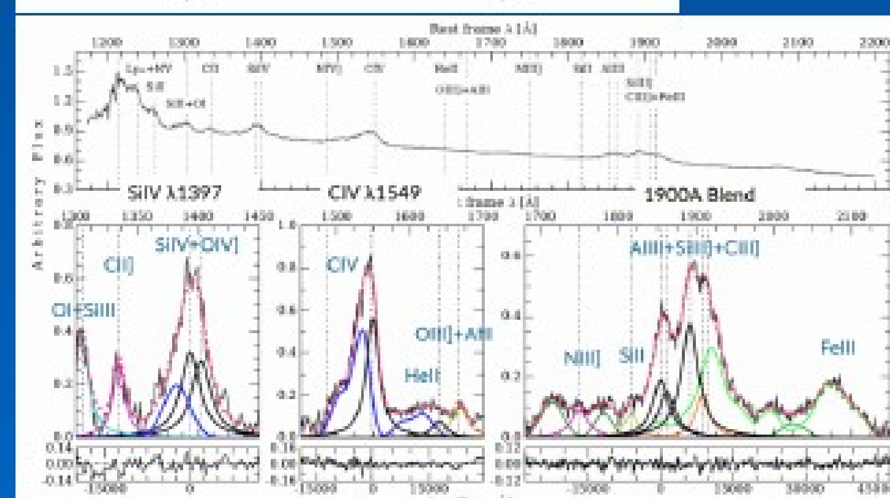

EXTREMNA POPULACIJA A – SELEKCIJA I FIZICKI USLOVI

xA sources enriched by a circumnuclear Starburst; the "first" unobscured stage emerging from an obscured evolution?

xA quasars can be **powerful radio sources, but radio power is "thermal" in origin implying SFR up to $\lesssim 10^3$ M$_\odot$**

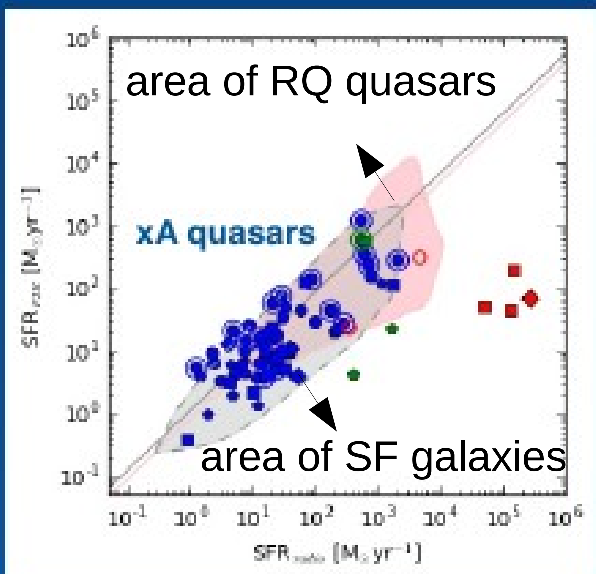

Extreme values for density (high, $n > 10^{12}$-10^{13} cm^{-3}), **ionization** (low, U~10^{-3}-$10^{-2.5}$), **metallicity** ($Z > 20\ Z_\odot$) or peculiar metallicity with anomalies in Al; radiation forces removed low-density gas?

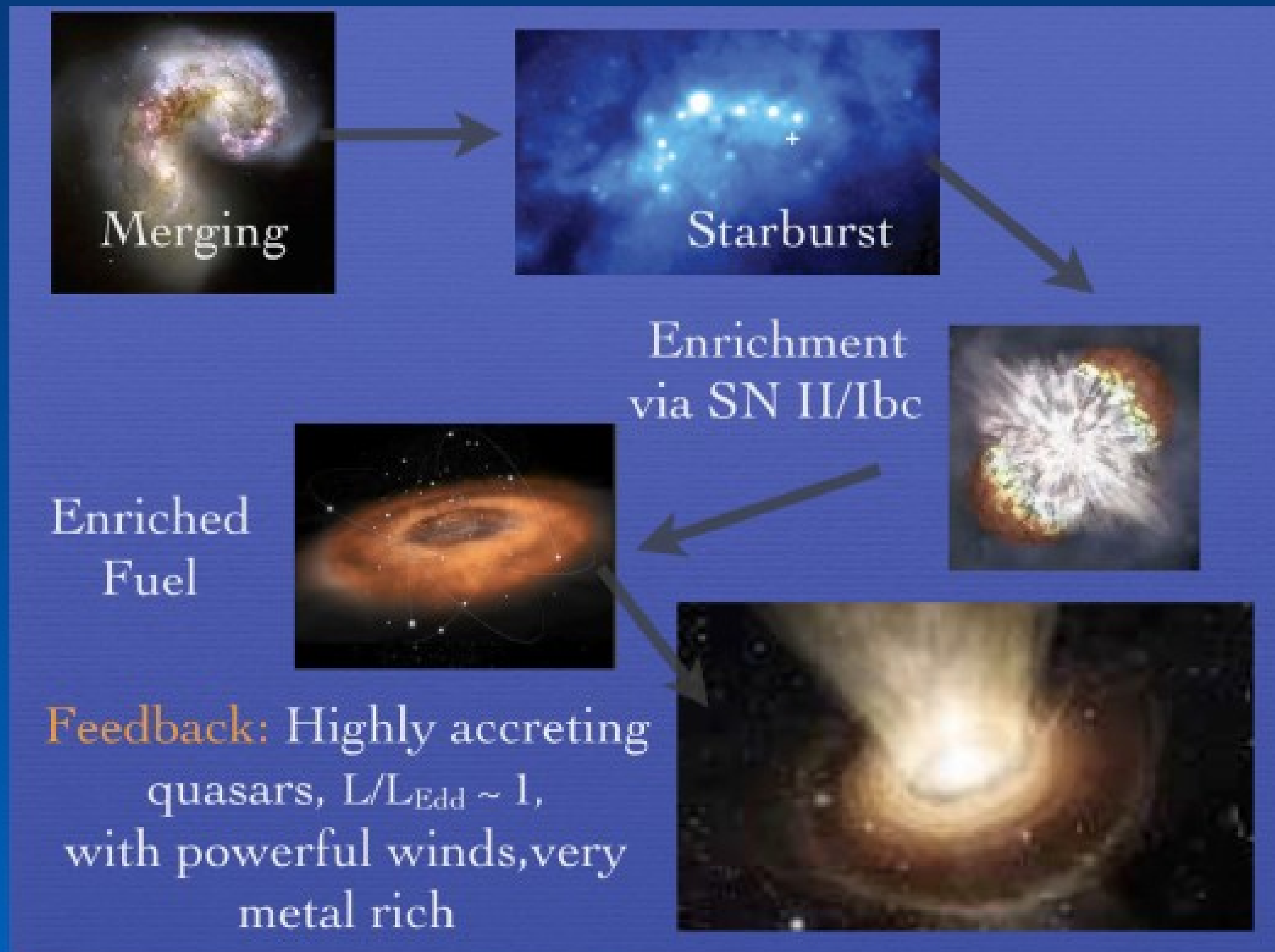

Ngrete et al. 2012; Martinez-Aldama et al. 2018; Ganci et al 2019
Sniegowska et al. 2019 in preparation; D'Onofrio & Marziani 2018, and references therein
more in the poster by del Olmo et al.

EXTREMNA POPULACIJA A – EDINGTONOVE STANDARDNE SVECE?

Extremely radiating quasars (xAs) are the quasars with the highest radiative output per unit black-hole mass, close to their Eddington limit. Accretion disk theory: low radiative efficiency at high accretion rate; L/L_{Edd} saturates toward a limiting value

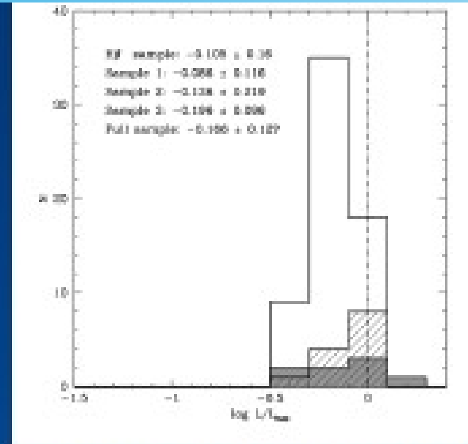

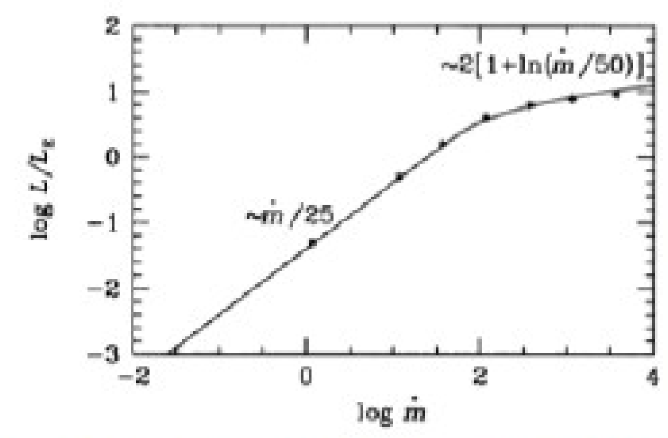

Marziani & Sulentic 2014 (MS14); Mineshige 2000; Abramowicz et al. 1988; Sadowski 2014

xA quasars radiate close to Eddington limit η~1 with small dispersion

$$L = \eta L_{\rm Edd} = {\rm const}\,\eta M_{\rm BH}$$

2. **Virial motions of the low-ion.** BLR, $L \propto \eta M_{BH} \propto \eta\ r_{BLR} (\delta v)^2$

$$M_{\rm BH} = \frac{f r_{\rm BLR} (\delta v)^2}{G}$$

3. **xA quasars show spectral invariance,** implying that the BLR radius rigorously scales as $r_{BLR} \propto [L/(n_H U)]^{1/2}$ (U and n_H constant)

➜ Virial Luminosity: $L \propto FWHM^4(H\beta)$

fraction of ionizing luminosity

$$L \approx 7.8\ 10^{44} \frac{\eta_1^2 \kappa_{0.5} f_2^2}{\bar{\nu}_{i2.42\ 10^{16}}} \frac{1}{(nU)_{9.6}} \delta v_{1000}^4 \ \ {\rm erg\ s^{-1}}$$

average frequency of ionizing photons

Significant constraints on Ω_M (0.30±0.06), better than supernovae, because of the z~2 coverage

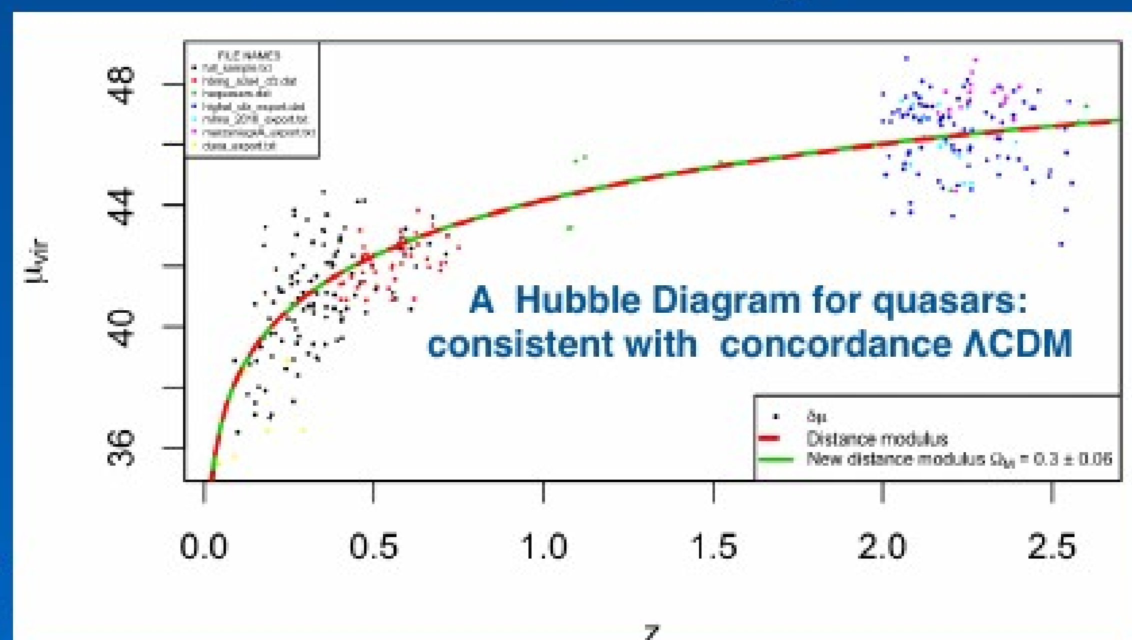

QUASARS IN COSMOLOGY

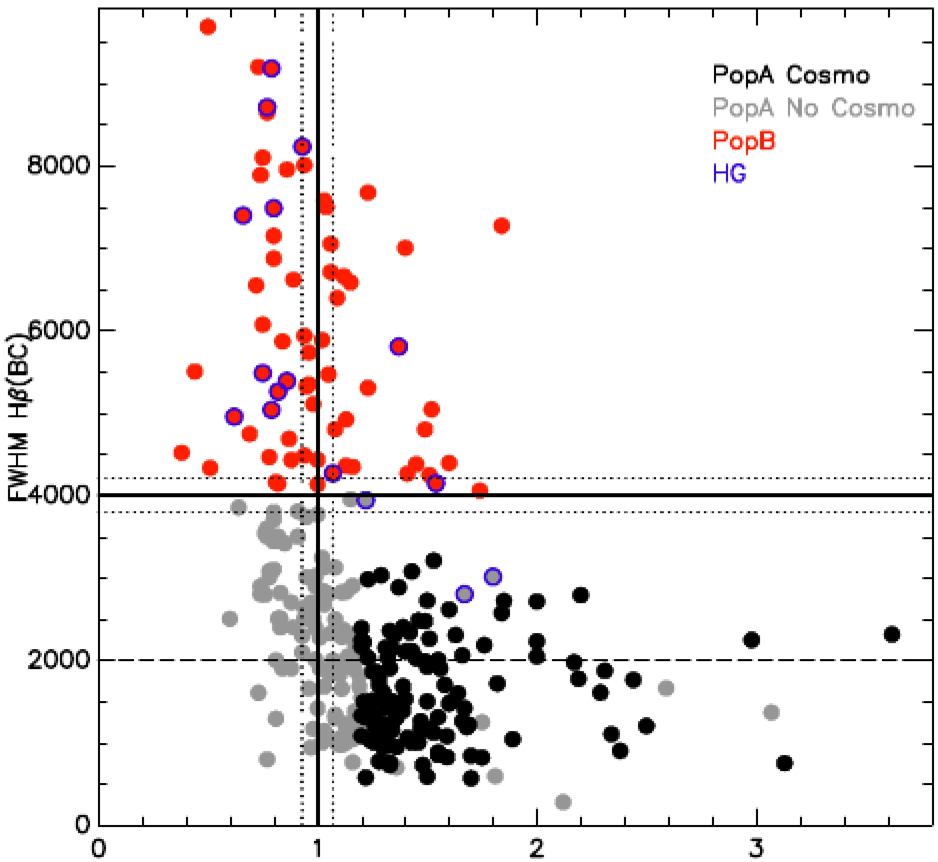

Fig. 1. Optical plane of the 4DE1 parameter space, FWHM(Hβ) vs. $R_{\rm FeII}$, for the present sample. Black dots indicate sources chosen for the "Cosmo" sample, i.e., with $R_{\rm FeII} \geq 1.2$, Grey dots the remaining Pop. A sources. Pop.B sources are indicated in red. A blue contour identifies sources with weak host-galaxy contaminations in their spectrum (HG). Vertical line separates the objects with $R_{\rm FeII} > 1$. This criteria is used to identify the extreme accretors. The filled horizontal line separates populations A and B, according Sulentic et al. (2000). Dotted lines indicates the typical error associated to $R_{\rm FeII}$ and the FWHM(Hβ). Dashed horizontal line delimits the region of NLSy1s (FWHM(Hβ) < 2000 km s^{-1}).

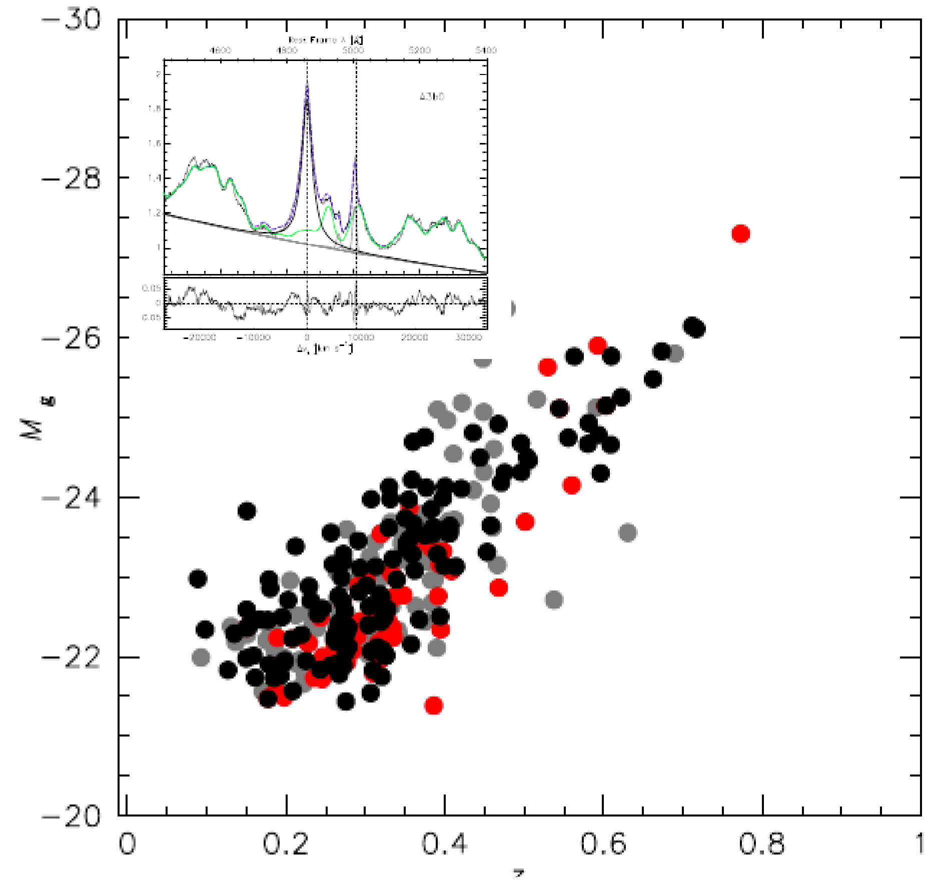

Fig. 3. Hubble diagram M_g vs. z for the 302 sources analyzed in this paper. Black circles: cosmo sample, grey circles: Pop. A not belonging to cosmo sample, red circles: Population. B. The cross indicates the average error.

Negrete, A. & Extreme Team A&A, 2018, 620,118

EXTREMNA POPULACIJA A – EDINGTONOVE STANDARDNE SVECE?

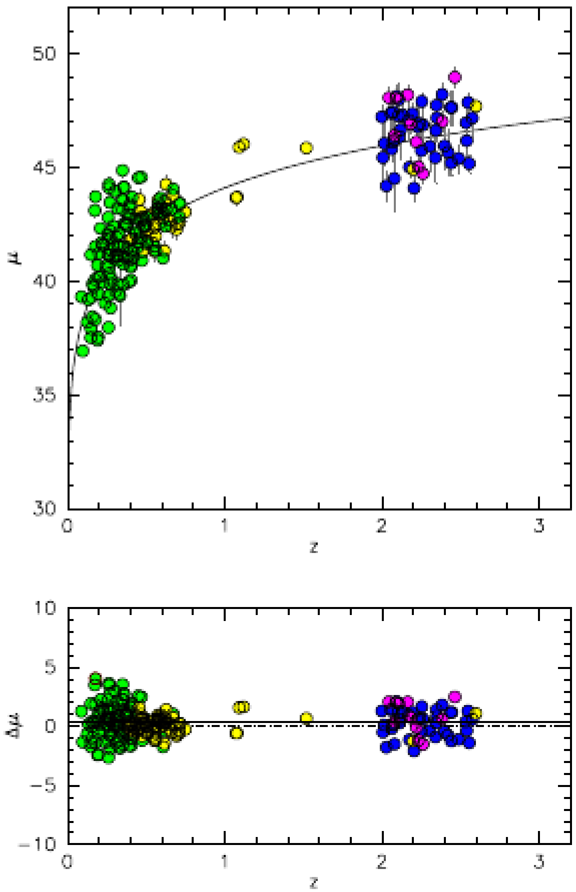

Fig. 20. Hubble diagram obtained from the analysis of the MS14 data (yellow: Hβ, navy blue: AlIIIλ1860 and SiIII]λ1892) supplemented by new Hβ measurements from the SDSS obtained in this work (green) and from GTC observations of Martínez-Aldama et al. (2018) (magenta). The lower panel shows the distance modulus residuals with respect to concordance cosmology. The filled lines represents a lsq fit to the residuals as a function of z.

Negrete, A. & Extreme Team A&A, 2018, 620,118

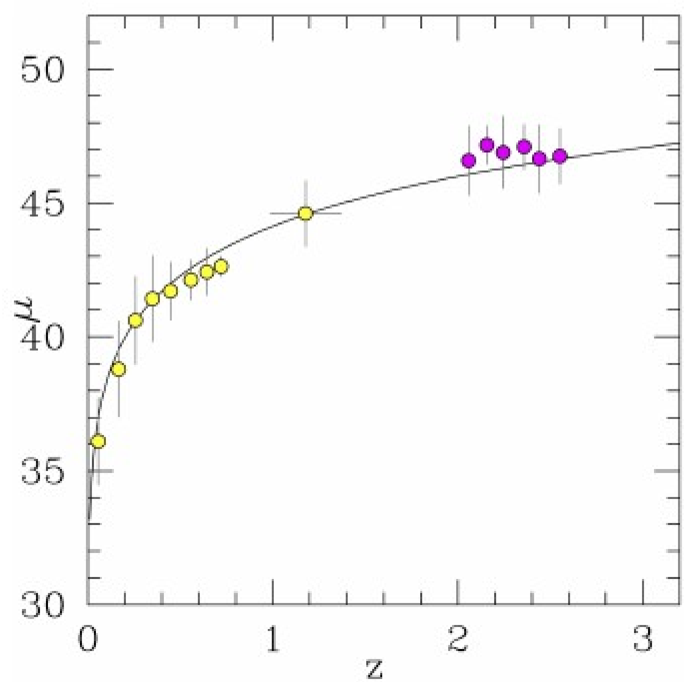

Marziani, P. & Extreme Team, 2019 IAU proceedings, Addis Ababa

KVAZARI KAO STANDARDNE SVECE

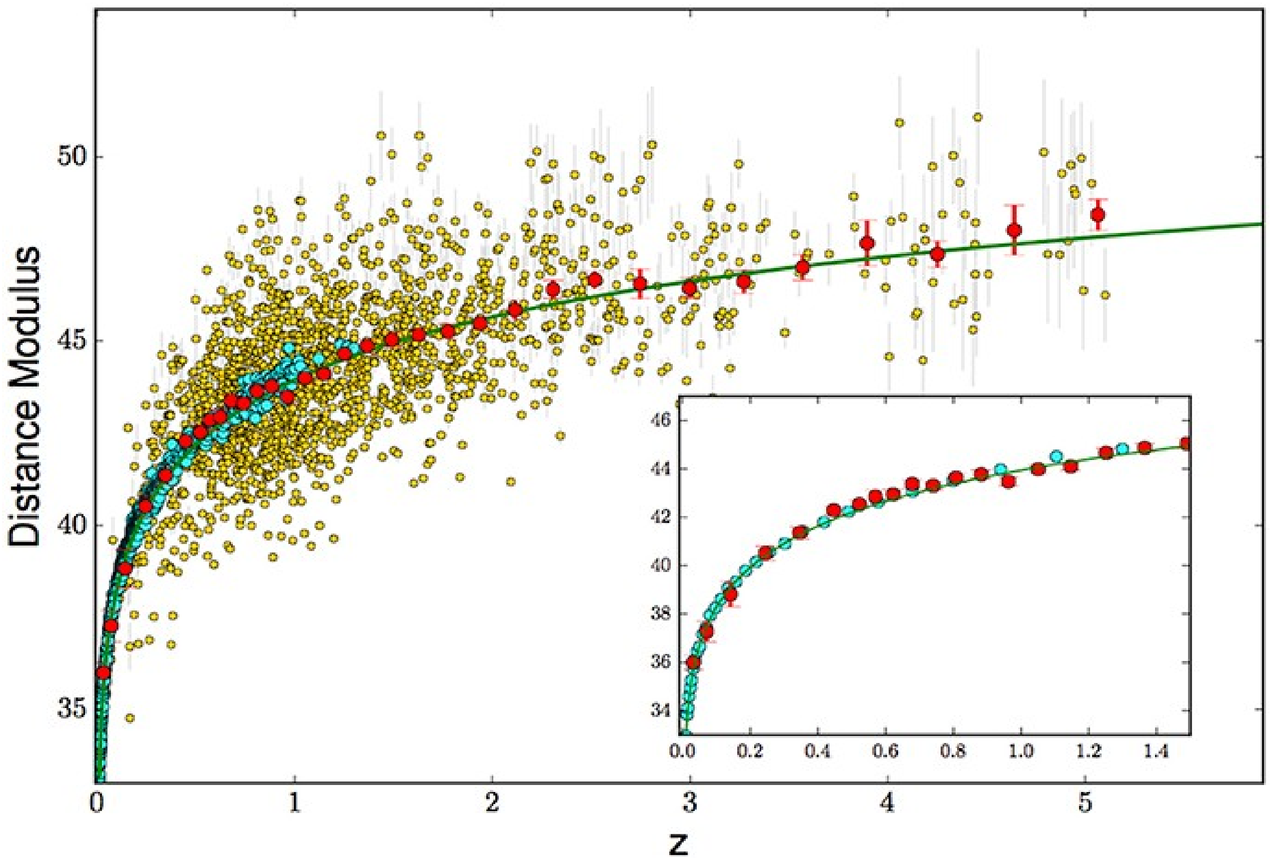

Risaliti+ introduced a new method to measure the cosmological parameters: they show that quasars can be used as “standard candles” by employing the non-linear relation between their intrinsic UV and X-ray emission as an absolute distance indicator.

Hubble diagram of quasars obtained with our “clean” sample and supernovae 1A. The orange points are single measurements for quasars, while the red points are quasar averages in small redshift bins. Type 1A supernovae are also plotted with cyan points (JLA sample, Betoule et al., 2014). The inset plot shows a zoom of the same diagram in the redshift range where supernova 1A and quasars overlap. In this case both red and cyan points are averages in small redshift bins for quasars and supernovae 1A respectively.

Bisogni S.,Risaliti G., Lusso E.2018, Frontiers in Astonomy

PROBLEMI AUTOMATSKE SELEKCIJE xA OBJEKATA

Example of spectra where host galaxy spectra mim
strong FeII emission leading to mistaken
identification of strong FeII emitters.
The panel show (from top to bottom):
-the real spectra and the best fitting model;
-the smoothed spectra overlapped with the best fitti
model,
-single stellar population spectra that was used in
the best fitting model, and
-the FeII template used in the fit.

Some prominent absorption lines are
marked on the plot.

SOURCES WITH STRONG HG CONTAMINATION

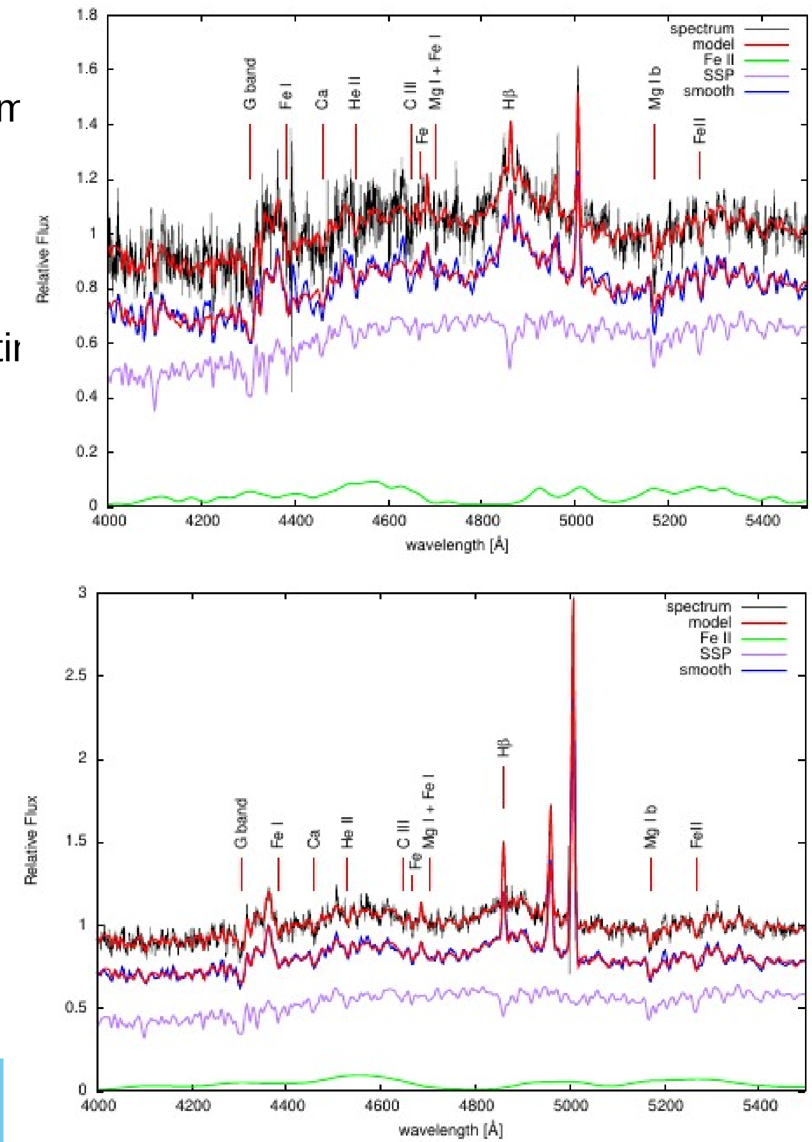

Bon, N. & Extreme Team, 2019, accepted for publication in A&A

DATA ANALYSIS

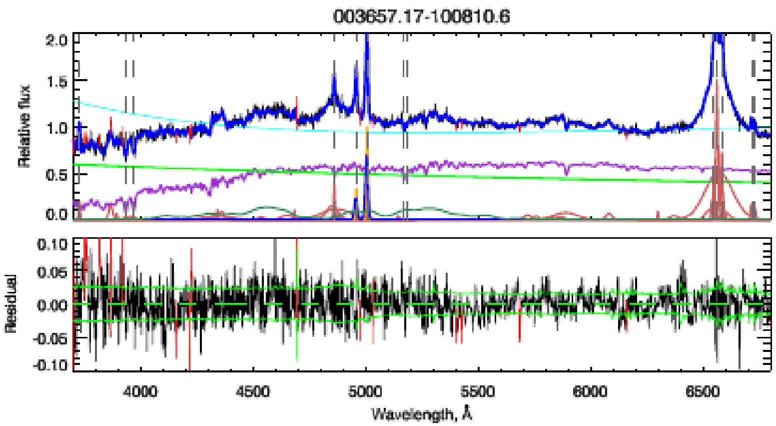

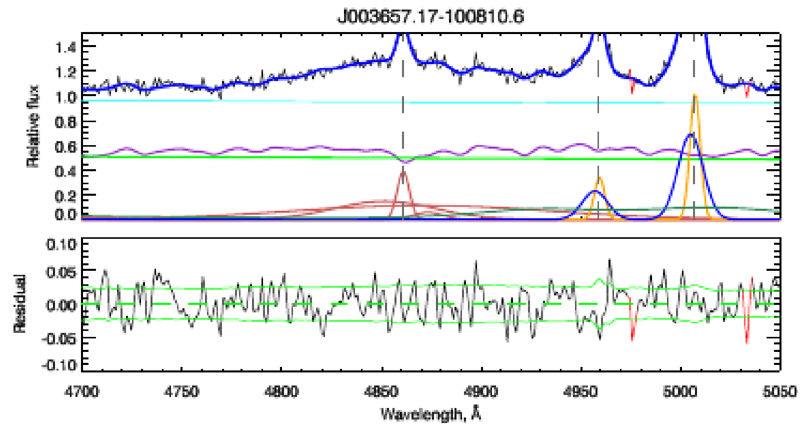

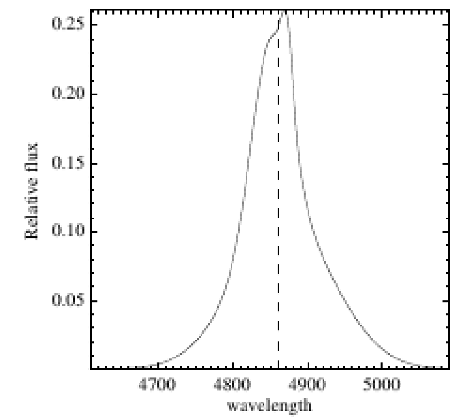

Spectra were carefully analysed with UlySS code (Koleva et al. 2009).

Components of the model:
-power low continuum (AGN continuum)
-single stellar population (PEGASE.HR)
-FeII template of Marziani et al. 2009
-Gaussian representation of emission line components

DATA ANALYSIS

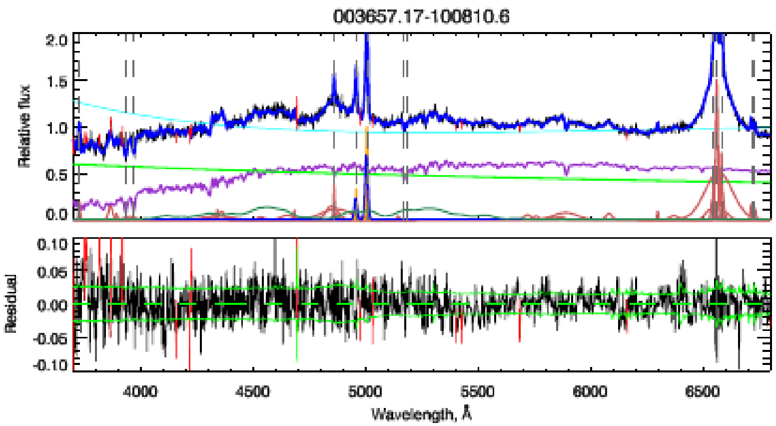

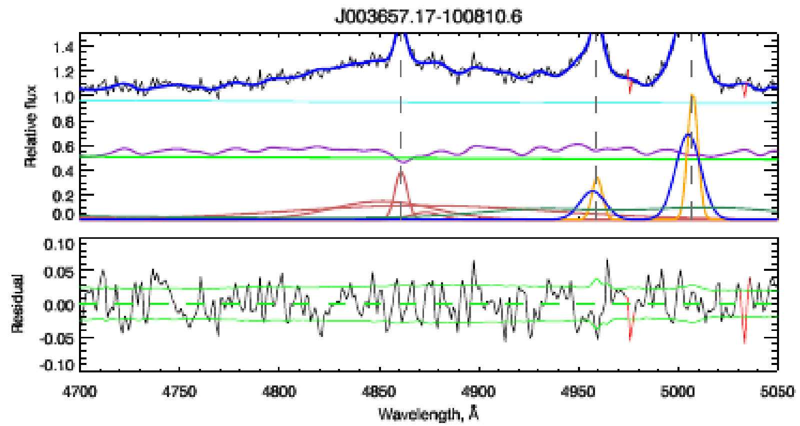

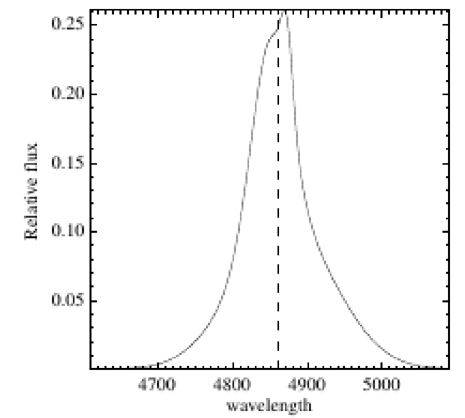

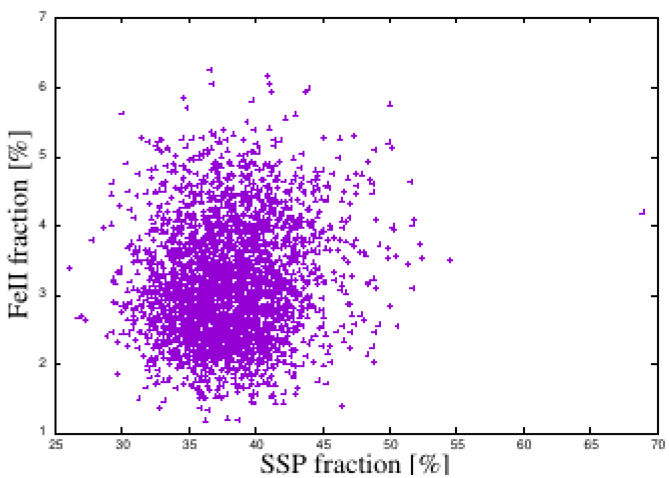

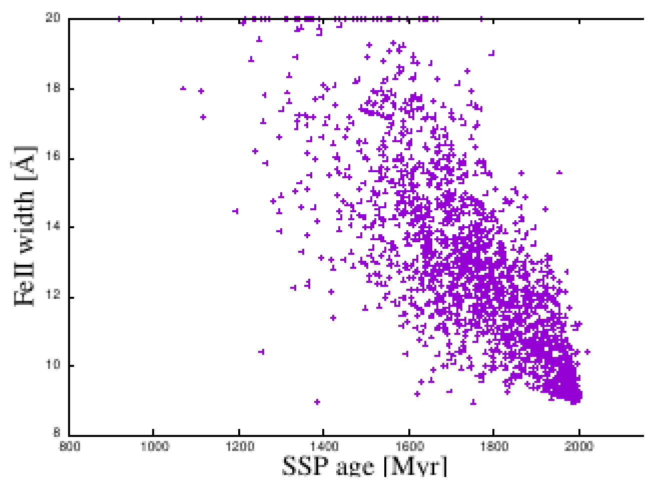

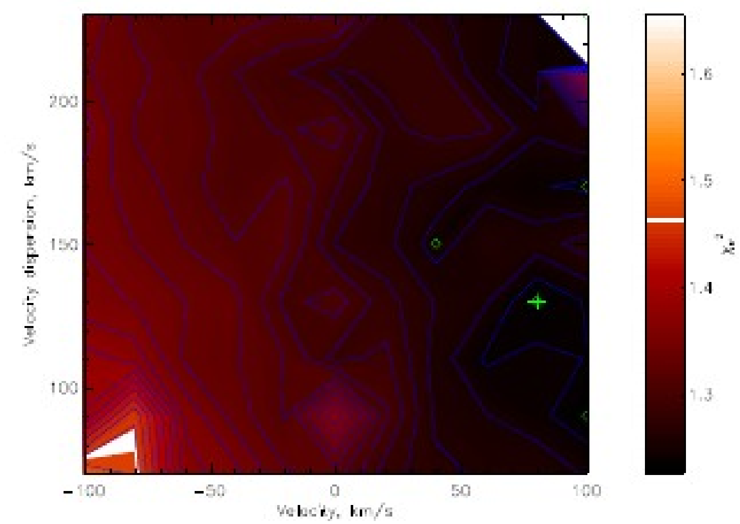

Bon, N. & Extreme Team, 2019, accepted for publication in A&A

PROBLEMS OF AUTOMATIC IDENTIFICATION OF EXTREME ACCRETING SOURCES

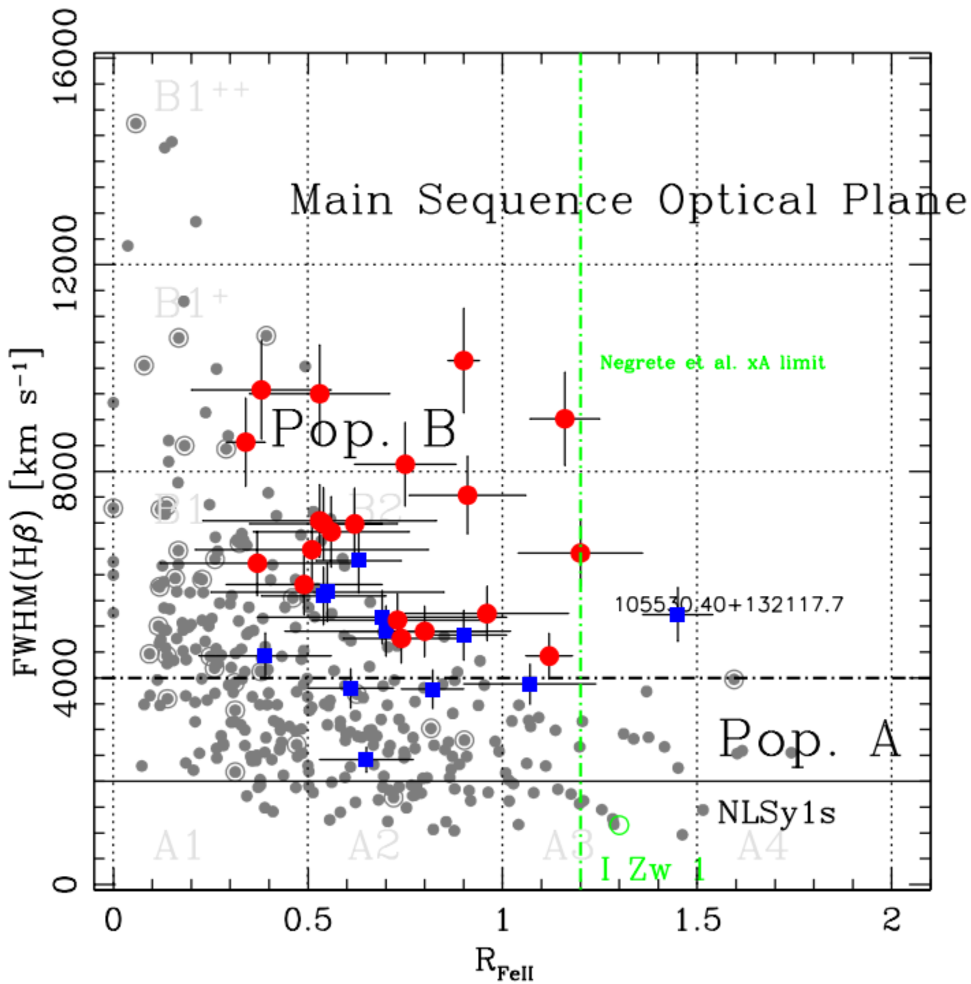

The optical plane of the E1 MS, FWHM HβBC vs. R_{FeII} .

The red circles are sources with the D parameter larger than 1.5; for the blue squares D . 1.5. The green line identifies the RFeII =1.2 limit for xA “safe” identification according to Negrete et al. 2018.

Bon, N. & Extreme Team, 2019, accepted for publication in A&A

Only one source is confirmed as xA in the full HG (host galaxy) sample (32 objects) after SSP analysis, and applying the selection criterion $R_{FeII} \geq 1.2$:

an object SDSSJ105530.40+132117.7

Consistency between AGN emission and host galaxy absorbion spectrum

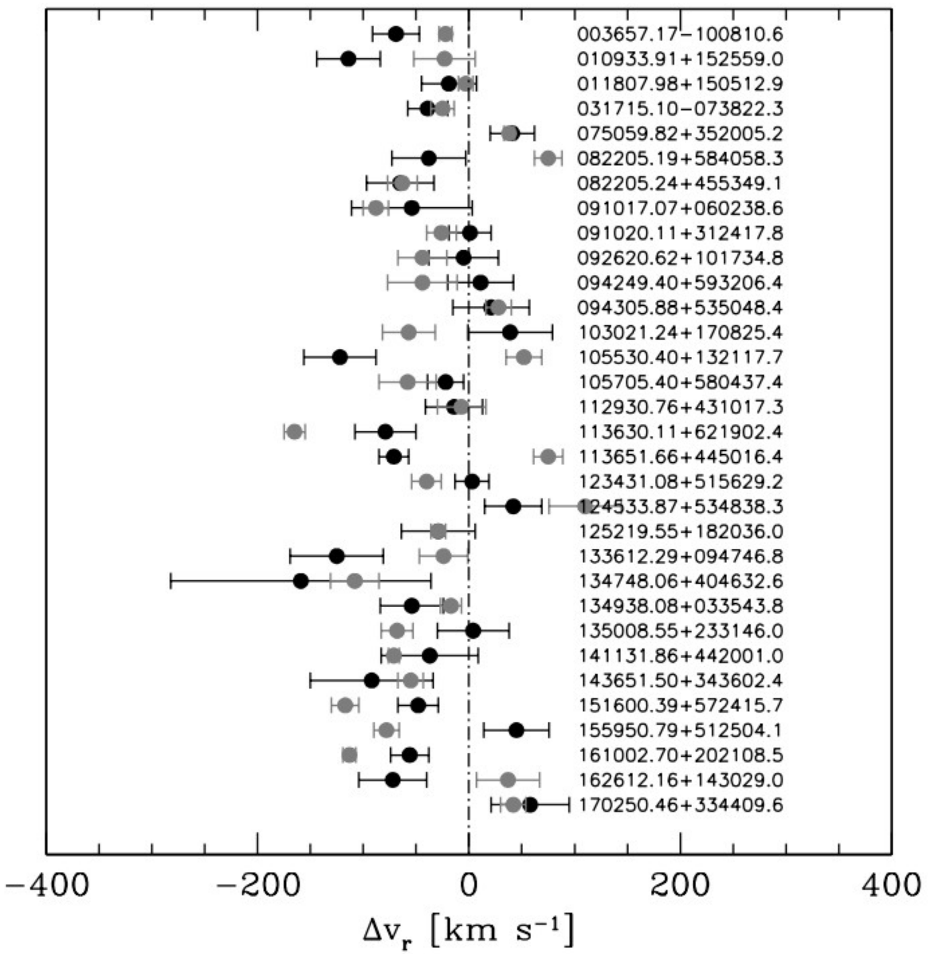

Radial velocity difference between HβNC (grey) and [OIII]λλ4959,5007 (black) with respect to the HG reference frame.

The comparison shows that both Hβ and [OIII]λλ4959,5007 shifts are consistent with HG with some scatter (54 km/s for the case of Hβ and 61 km s−1 for [OIII].

The Pearson's cross-correlation between parameters pointed out the high cross-correlation coefficient (r=0.62, P-value=4.83E-05) between the shift of narrow component of Hβ line and SSP cz. On the other hand we did not find the expeted correlation between the SSP cz and the shift of narrow component of [OIII]4959,5007 lines.

Bon, N. & Extreme Team, 2019, accepted for publication in A&A

Method to derive emissivity weighted n_e

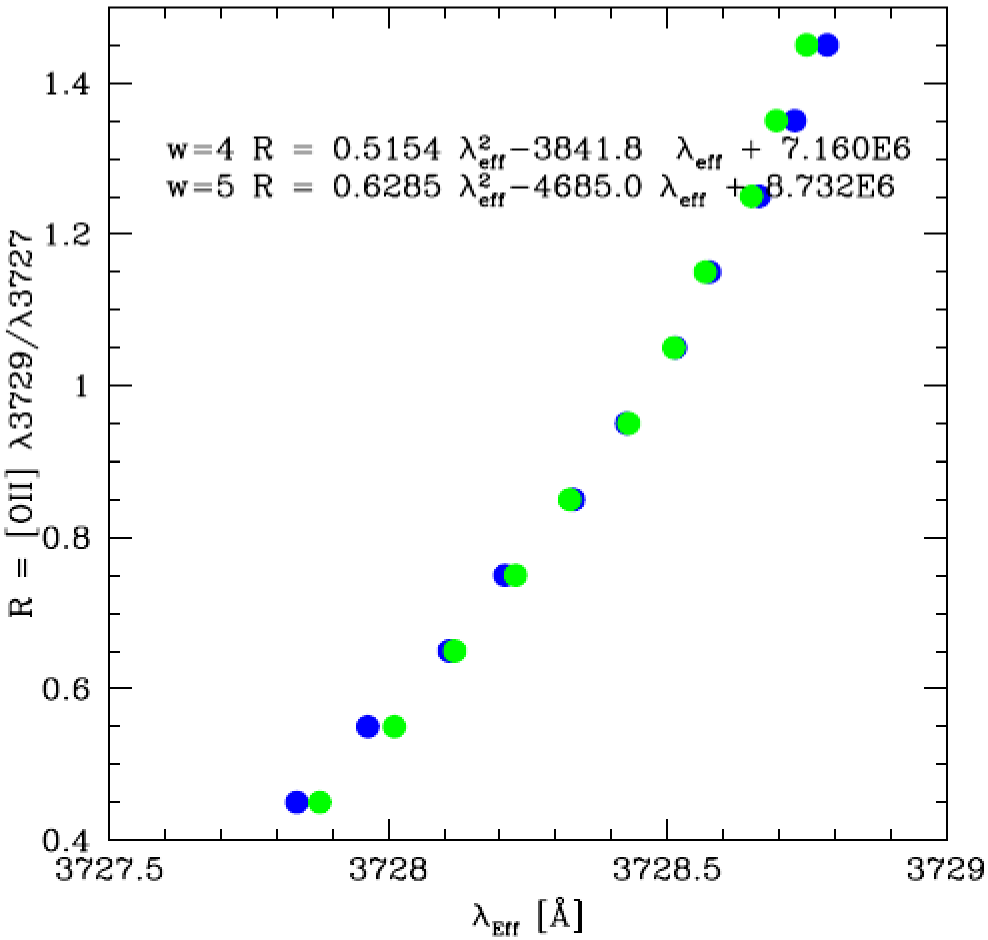

R=[OII]λ3729/λ3726 as a function of [OII]λλ3726,3729 doublet effective wavelength for an unresolved mock doublet of 4 and 5 Å.
Green spots correspond to the case w=5.

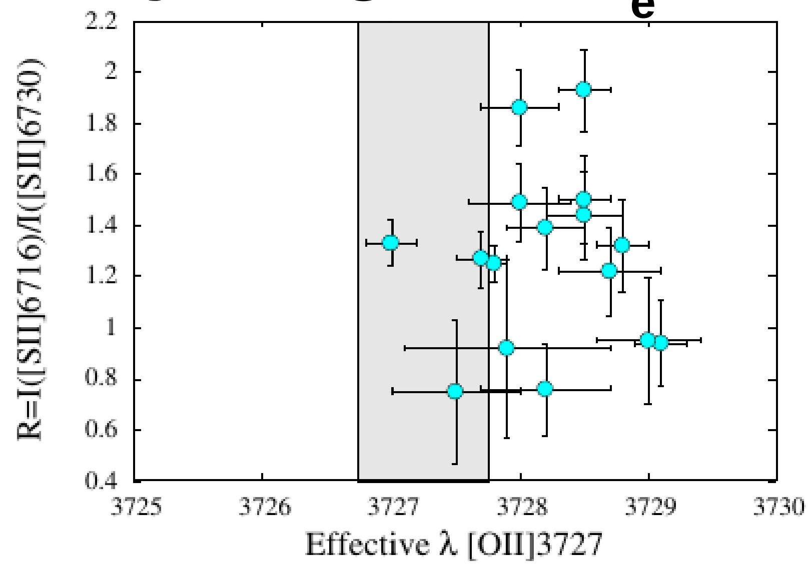

Spectra must be de-shifted for SSP cz!

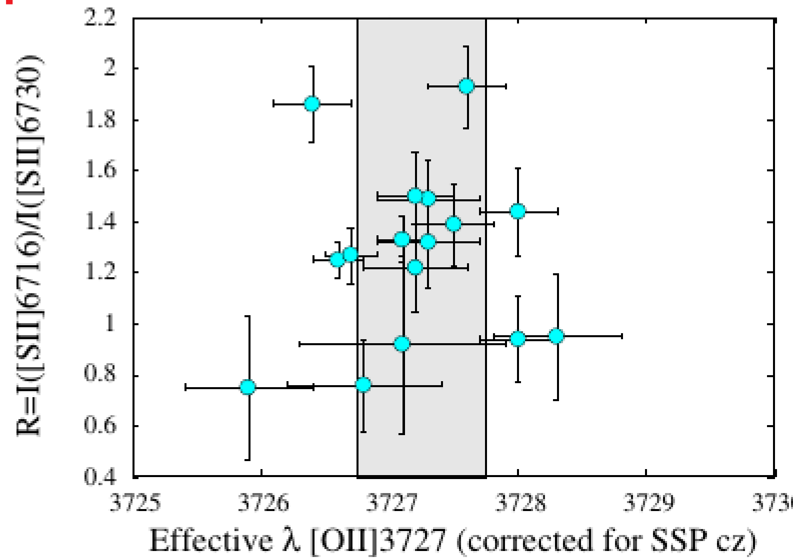

The intensity ratio [SII]λ6717/λ6731 as a function of [OII]λλ3726,3729 doublet effective wavelength for unresolved doublets: [OII]λλ3726,3729 doublet effective wavelength not corrected (top); corrected for SSP cz (bottom). Region inside the physical limits of the effective wavelengths of [OII]λ3727 is shaded on the plots.

n_e retrieved is mainly consistent with NLR density, except in two cases when we obtained the significantly lower density.

No strong outflows diagnosed by the [OIII] profile

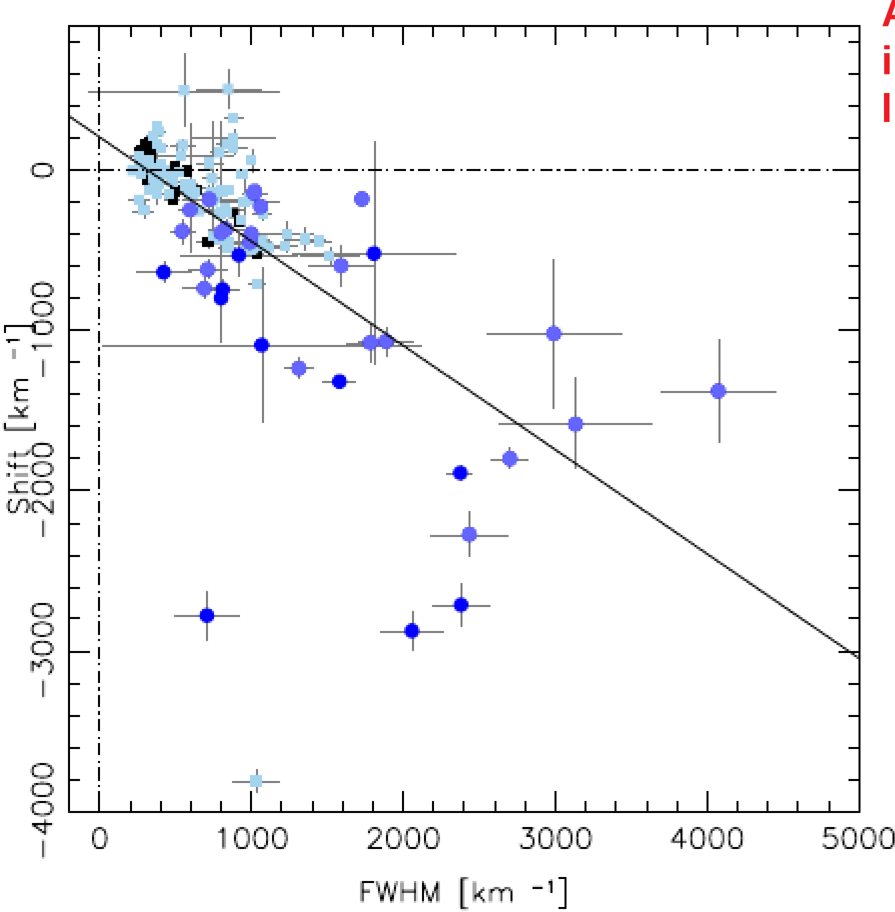

Shifts vs. FWHM for the Pop. A objects. For the objects in which both [OIII] NC+SB were fitted, the black squares represents the NC while the SB component is in light blue circles. The sources fitted with a single NC are plotted in pale blue squares, while the ones with only a SB component are represented by darker blue circles (Negrete & Extreme Team 2018.)

As for typical type 1 AGN, the distrubution of the sources in our sample is skewed to the blue, especially toward the line base. The amplitude of the blueshifts is however modest.

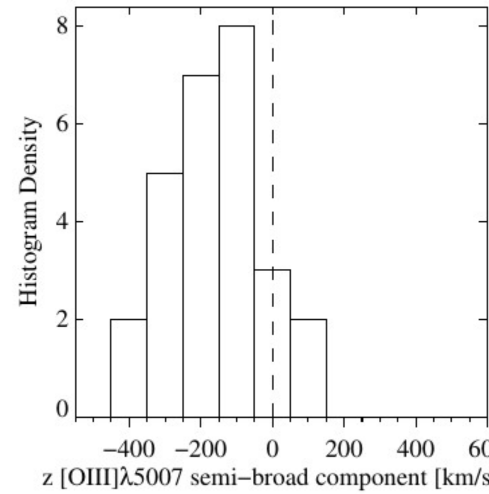

Distribution of the shift of [OIII]λ5007 semi-broad component.

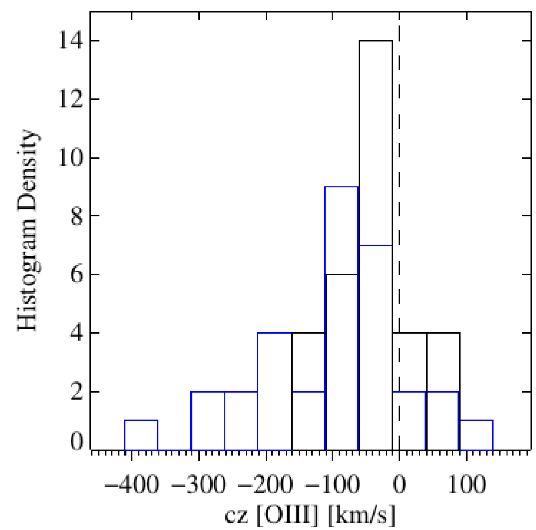

Distribution of the c(1/4) [OIII]λ5007 (blue) and of the c(0.9) [OIII]λ5007.

ZAKLJUČCI

The MS offer contextualization of quasar observational and physical properties.

The differences between Population A and B (“wind-“ and “disk-dominated,” respectively) might be associated with a change of accretion mode (from geometrically thin, optically thick to slim disk?), as several properties appear to change at $L/L_{Edd} \sim 0.1 - 0.2$.

A proper identification of xA sources requires a carefull multicomponent fit, that includes the spectrum of the host galaxy, especially if the AGN is of low luminosity.

It is necessary to perform a simultaneous multicomponent fit in order to retrieve information on the stellar component and on the FeII emission. Inclusion of the spurious xA sources may dramaticaly increase the dispersion in the Hubble diagram of quasars obtained from virial luminosity estimates.

Extreme Population A (xA) quasars at the high R_{FeII} end of the MS appear to radiate at extreme L/L_{Edd}. xA quasars show a relatively high prevalence (10%) and are easily recognizable.

xA quasars might be suitable as “Eddinton standard candels”